Wear 426–427 (2019) 620–636

Contents lists available at ScienceDirect

Wear

journal homepage: www.elsevier.com/locate/wear

Review of the API RP 14E erosional velocity equation: Origin, applications, misuses, limitations and alternatives

F. Madani Sani[a,*], S. Huizinga[b], K.A. Esaklul[c], S. Nesic[a]

[a] Ohio University, USA
[b] Sytze Corrosion Consultancy, The Netherlands
[c] Occidental Petroleum Corporation, USA

ARTICLE INFO

Keywords:
API RP 14E
Erosional velocity
Velocity limit
Erosion
Sand erosion
Erosion-corrosion

ABSTRACT

Oil and gas companies apply different methods to limit erosion-corrosion of mild steel lines and equipment during the production of hydrocarbons from underground geological reservoirs. One of the frequently used methods is limiting the flow velocity to a so-called "erosional velocity", below which it is assumed that no erosion-corrosion would occur. Over the last 40 years, the American Petroleum Institute recommended practice 14E (API RP 14E) equation has been used by many operators to estimate the erosional velocity. The API RP 14E equation has become popular because it is simple to apply and requires little in the way of inputs. However, due to a lack of alternatives and its simplicity, the API RP 14E equation has been frequently misused by it being applied to conditions where it is invalid, by simply adjusting the empirical *c*-factor. Even when used within the specified conditions and associated applications, the API RP 14E equation has some limitations, such as not providing any quantitative guidelines for estimating the erosional velocity in the two most common scenarios found in the field: when solid particles are present in the production fluids and when erosion and corrosion are both involved. A range of alternatives to the API RP 14E equation that are available in the open literature is presented. Some of these alternatives overlap with API RP 14E, while others go beyond its narrow application range, particularly when it comes to erosion by solid particles. A comparison between the experimentally obtained and calculated erosion by different models is presented. The erosional velocity calculated by some of the models was compared with that estimated by the API RP 14E equation.

1. Introduction

Erosion of carbon steel piping and equipment is a major challenge during production of hydrocarbons from underground geological reservoirs, becoming even more complicated when electrochemical corrosion is involved. With the need to maintain production rates, operators continuously drill deeper into such reservoirs and/or use proppants as well as other fracturing techniques. Thus, deeper aquifers are encountered, water cuts are increased, more multiphase streams are produced, and more solids and corrosive species are introduced into the production, transportation and processing systems, which in turn leads to increased erosion and erosion-corrosion problems [1–4].

The terms erosion and erosion-corrosion are often inadequately described and distinguished. For clarity, erosion is defined as pure mechanical removal of the base metal, usually due to impingement by solid particles, although liquid droplet impingement and bubble collapse impacts can cause the same type of damage [5–7]. Corrosion is considered to be an (electro)chemical mode of material degradation, where metal oxidatively dissolves in a typically aqueous environment. Corrosion can be enhanced by intense turbulent flow; in this case it is called flow induced corrosion (FIC) or flow accelerated corrosion (FAC) [8–11]. Erosion-corrosion is a combined chemo-mechanical mode of attack where both erosion and corrosion are involved [7,12,13]. The resulting erosion-corrosion rate can be larger than the sum of individual erosion and corrosion rates, due to synergistic effects between erosion and corrosion processes [14–18].

Oil and gas companies have always tried to develop appropriate methods to limit erosion-corrosion to an acceptable level [1,19,20]. One of the commonly used methods is reducing the flow velocity below a so-called “erosional velocity” limit, where it is thought that no metal loss would occur below this velocity [1,21,22]. However, there have been persistent concerns about the validity and accuracy in

* Correspondence to: Institute for Corrosion and Multiphase Technology, Department of Chemical and Biomolecular Engineering, Ohio University, 342 W State St., Athens, OH 45701, USA.
E-mail addresses: fm874012@ohio.edu, fazlollah.madani.sani@gmail.com (F. Madani Sani).

https://doi.org/10.1016/j.wear.2019.01.119
Received 24 October 2018; Received in revised form 16 January 2019; Accepted 20 January 2019

Nomenclature

Normal letters

A_i	Empirical constant, Eq. (42)
A_{pipe}	Cross sectional area of pipe (m^2), Eq. (24)
A_t	Area exposed to erosion (m^2), Eqs. (24), (27)
C_1	Model geometry factor, Eqs. (25), (27)
C_{std}	r/D of a standard elbow (assumed to be 1.5), Eq. (30)
C_{unit}	Unit conversion in Eq. (27) (3.15×10^{10}), Eqs. (26), (27)
D'	Standard particle diameter (μm), Eq. (36)
D_{eff}	Effective pipe diameter, Eq. (53)
D_o	Reference pipe diameter (1″ or 25.4 mm), Eqs. (28), (40)
D_P	Particle diameter (μm), Eq. (36)
E_{90}	A unit of material volume removed per mass of particles at 90° (mm^3/kg), Eqs. (35), (36)
$E_{L,y}$	Annual surface thickness loss (mm/year), Eq. (27)
E_L	Erosion rate or annual surface thickness loss (mm/year), Eq. (17)
E_m	Material loss rate (kg/s), Eq. (15)
F_M	Empirical constant that accounts for material hardness, Eqs. (28), (29)
F_P	Penetration factor for material based on 1″ (25.4 mm) pipe diameter (m/kg), Eqs. (28), (40)
$F_{r/D}$	Penetration factor for elbow radius of curvature, Eqs. (28), (30)
F_s	Empirical particle shape coefficient, Eqs. (28), (39)
H_V	Material's initial Vicker's hardness (GPa), Eqs. (36), (38), (41), (43)
K_s	Fitting erosion constant, Eq. (13)
L_o	Reference equivalent stagnation length for a 1″ ID pipe (in), Eqs. (31), (32)
Q_G	Volumetric flow rate of gas, Eq. (53)
Q_L	Volumetric flow rate of liquid, Eq. (53)
S_g	Gas specific gravity at standard conditions, (air = 1) Eq. (2)
S_l	Liquid specific gravity at standard conditions (water = 1); use average gravity for hydrocarbon-water mixtures), Eq. (2)
	Geometry-dependent constant, Eq. (14)
U_P	Particle impact velocity (m/s) (equal to the mixture fluid velocity), Eqs. (15), (17), (19), (27)
V'	Standard particle impact velocity (m/s), Eq. (36)
V_e	Fluid erosional velocity (ft/s), Eqs. (1), (3), (13)
V_f	Fluid velocity along the stagnation zone, Eqs. (33), (34), (50), (51)
V_L	Characteristic particle impact velocity (m/s), Eqs. (28), (39)
V_m	Fluid mixture velocity (m/s) ($= V_{SG} + V_{SL}$), Eq. (14)
V_m	Mixture velocity, Eq. (46)
V_o	Fluid bulk (average) velocity (flow stream velocity), Eqs. (34), (46), (47)
V_P	Particle velocity along the stagnation zone, Eqs. (33), (50)
V_P	Particle impact velocity (m/s), Eq. (36)
V_{SG}	Superficial gas velocity, Eqs. (44)-(49)
V_{SL}	Superficial liquid velocity, Eqs. (44)-(49)
$d_{P,c}$	Critical particle diameter (m), Eq. (21)
d_P	Particle diameter (m), Eqs. (22), (30)
d_P	Particle diameter, Eqs. (33), (51), (52)
m_P	Mass rate of particles (kg/s), Eqs. (15), (17), (27)
n_1, n_2	Empirical exponents, Eqs. (37), (38)
n_1, n_2, n_3	Empirical exponents, Eq. (43)
q_s	Solid (sand) flow rate (ft^3/day), Eq. (13)
s_1, q_1, s_2, q_2	Empirical parameters, Eq. (38)
u_M	Mean velocity of two-phase mixture (m/s), Eq. (4)
A	Minimum pipe cross-sectional flow area required (in^2/1000 barrels liquid per day), Eq. (3)
A	Cross-sectional area of the pipe (ft^2), Eq. (6)
A	Dimensionless parameter group, Eqs. (19), (21)
B	Brinell hardness (B), Eqs. (29), (39), (41)
C	Empirical constant, Eq. (29)
C	Empirical constant, Eq. (39)
D	Pipe internal diameter (mm), Eq. (14)
D	Inner pipe diameter (m), Eqs. (17), (19), (21), (22), (24)
D	Pipe diameter (in or mm), Eqs. (28), (40)
D	Ratio of pipe diameter to 1-in pipe, Eq. (30)
D	Pipe inner diameter (in), Eqs. (31), (32)
$E(\alpha)$	A unit of material volume removed per mass of particles at arbitrary angle α (mm^3/kg), Eq. (35)
ER	Erosion rate (penetration rate) (mm/y), Eq. (14)
ER	Erosion ratio (kg/kg), Eqs. (39), (40)
$F(\theta)$	Impact angle function, Eqs. (39), (42), (43)
$F(\alpha)$	Impact angle function, Eqs. (15), (16), (27)
G	Correction function for particle diameter, Eqs. (23), (27)
GF	Geometry factor, Eq. (27)
ID	Pipe inner diameter, Eq. (53)
K	High-speed erosion coefficient (≅ 0.01), Eq. (6)
K	Material erosion constant ($(m/s)^{-n}$), Eqs. (15), (27)
K, k_1, k_2, k_3	Empirical coefficients, Eq. (36)
L	Stagnation length (in), Eqs. (31), (32), (34), (52)
P	Operating pressure (psia), Eqs. (2), (3)
P	Target material hardness (psi) ($= 1.55 \times 10^5$ psi for steel), Eq. (6)
R	Gas/liquid ratio at standard conditions (ft^3/barrel) (1 barrel assumed to be 5.61 ft^3), Eqs. (2), (3)
R	Radius of curvature of elbow (Reference of radius of curvature is centerline of pipe), Eq. (18)
Re	Particle Reynolds number, Eqs. (50), (51)
T	Operating temperature (°R), Eqs. (2), (3)
V	Fluid velocity (ft/s), Eq. (5)
V	Impact velocity of the fluid (ft/s), Eq. (6)-(8)
V	Velocity to remove the corrosion inhibitor film from the surface (ft/s), Eqs. (9), (10)
V	Maximum velocity of gas to avoid noise (m/s), Eq. (11)
V	Maximum velocity of mixture (m/s), Eq. (12)
W	Sand flow rate (kg/day), Eq. (14)
W	Sand production rate (kg/s), Eqs. (28), (40)
c	Empirical constant ($\sqrt{(lb/(ft\,s^2))}$), multiply by 1.21 for SI units, Eq. (1)
d	Pipe inner diameter (in), Eq. (13)
d	Sand size (μm), Eq. (14)
f	Friction factor, Eq. (9)
f	Maximum value of $F(\theta)$, Eq. (43)
g	Gravitational constant (32.2 ft/s^2), Eqs. (6), (9)
$g(\alpha)$	Impact angle function, Eqs. (35), (37)
h	Erosion rate (mpy), Eq. (6)
h	Penetration rate (m/s), Eqs. (28), (40)
i	Empirical exponent, Eq. (42)
n	Velocity exponent, Eqs. (15), (27)
r	Elbow radius of curvature (a multiple of D) (*e.g.* 5D), Eq. (30)
x	Particle location along the stagnation zone, Eqs. (33), (34)

Greek letters

γ_c	Critical ratio of particle diameter to geometrical diameter, Eqs. (21), (23)
μ_f	Fluid viscosity (pa-s), Eq. (30)
μ_f	Fluid dynamic viscosity, Eqs. (33), (51)
μ_G	Gas phase dynamic viscosity, Eq. (45)

μ_L	Liquid phase dynamic viscosity, Eq. (45)	ρ_t	Density of target material (kg/m^3), Eq. (27)
μ_m	Viscosity of fluid mixture (kg/m-s), Eq. (19)	ϵ_c	Critical strain to failure (0.1 for steel), Eq. (6)
μ_m	Mixture dynamic viscosity, Eq. (45)	ΔP	Total pressure drop along the flow path (psi), Eq. (5)
ρ_f	Fluid density (kg/m^3), Eq. (30)	Z	Gas compressibility factor, Eqs. (2), (3)
ρ_f	Fluid density, Eqs. (33), (51), (52)	Φ	Dimensionless parameter (mass ratio), Eqs. (50), (52)
ρ_G	Gas phase density, Eq. (44)	α	Particle impact angle (rad), Eqs. (15), (16), (18), (19), (24), (27), (37)
ρ_L	Liquid phase density, Eq. (44)	β	Density ratio between particle and fluid, Eqs. (20), (21)
ρ_m	Gas/liquid mixture density at flowing pressure and temperature (lb/ft^3), Eqs. (1), (2)	γ	Ratio of particle diameter to geometrical diameter, Eqs. (22), (23)
ρ_M	Mean density of two-phase mixture (kg/m^3), Eq. (4)	θ	Impact angle (rad or degree), Eqs. (39), (42)
ρ_m	Fluid mixture density (kg/m^3) ($= (\rho_l V_l + \rho_g V_g)/V_m$), Eq. (14)	θ	Impact angle (rad), Eq. (43)
ρ_m	Density of fluid mixture (kg/m^3), Eqs. (19), (20)	ν	Impacting fluid volume rate (ft^3/s) ($= AV$), Eq. (6)
ρ_m	The density of mixture (kg/m^3), Eq. (12)	ρ	Fluid density (lb/ft^3), Eqs. (5) to (10)
ρ_m	Mixture density, Eq. (44)	ρ	Density of gas (kg/m^3), Eq. (11)
ρ_P	Density of particle (kg/m^3), Eqs. (19), (20)	τ	Shear strength of the inhibitor interface (psi), Eq. (9)
ρ_P	Particle density, Eqs. (33), (52)		

determination of this critical velocity, given the complexities of conjoint attack by erosion and corrosion. When the erosional velocity is estimated conservatively (to be too low), the companies inexcusably lose production; when it is determined too optimistically (to be too high) then they risk severe damage and loss of system integrity. One of the guidelines that has been used extensively over the last 40 years for estimating the erosional velocity is a recommended practice proposed by the American Petroleum Institute called API RP 14E [1,23,24].

API RP 14E was originally developed for sizing of new piping systems on production platforms located offshore that carry single or two-phase flow [25]. Overtime, the application of API RP 14E mostly shifted to estimation of the erosional velocity, so that it is typically acknowledged as the "API RP 14E erosional velocity equation" in the field of oil and gas production.

The widespread use of the API RP 14E erosional velocity equation is a result of it being simple to apply and requiring little in the way of inputs [26,27]. However, it is often quoted that the API RP 14E erosional velocity equation is overly conservative and frequently unjustifiably restricts the production rate or overestimates pipe sizes [28–30]. The present work provides a critical review of literature on the origin of the API RP 14E erosional velocity equation, its applications, misuses, limitations and finally lists a few alternatives.

2. Summary of API RP 14E

API RP 14E provides "minimum requirements and guidelines for the design and installation of new piping systems on production platforms located offshore". The API RP 14E offers sizing criteria for piping systems across three flow regimes: single-phase liquid, single-phase gas and two-phase gas/liquid. The API RP 14E sizing criteria for each category are briefly discussed below with a focus on how they relate to erosion-corrosion.

(1) Single-phase liquid flow lines
The primary basis for sizing single-phase liquid lines is *flow velocity* and *pressure drop*. It is recommended that the pressure should always be above the vapor pressure of liquid at the given temperature, in order to avoid cavitation that could lead to erosion. On the other hand, it is suggested that the velocity should not be less than 3 ft/s to minimize deposition of sand and other solids [25]; which presumably may lead to underdeposit corrosion attack. No other limiting criteria for determining flow velocity are mentioned that are related to either erosion or erosion-corrosion.

(2) Single-phase gas flow lines
For single-phase gas lines, *pressure drop* is the primary basis for sizing. Only a passing reference is made to a velocity limitation related to "stripping a corrosion inhibitor film from the pipe wall", which clearly points towards erosion-corrosion. However, no specific guidance is offered on how to determine this limitation [25].

(3) Gas/liquid two-phase lines
API RP 14E lists *erosional velocity* , *minimum velocity*, *pressure drop*, *noise*, and *pressure containment* as criteria for sizing gas/liquid two-phase lines. The guideline states that "flow lines, production manifolds, process headers and other lines transporting gas and liquid in two-phase flow should be sized primarily on the basis of flow velocity", what leads to the erosional velocity criterion. API RP 14E recommends that, "when no other specific information as to erosive or corrosive properties of the fluid is available", the flow velocity should be limited to the so-called "erosional velocity", above which "erosion" may occur. API RP 14E suggests the following empirical equation for calculating the erosional velocity [25]:

$$V_e = \frac{c}{\sqrt{\rho_m}} \tag{1}$$

Even though in the definition of the erosional velocity only erosion is mentioned, the recommended c-factors by the API RP 14E for Eq. (1) cover situations where both corrosion and erosion-corrosion are problematic. API RP 14E states that "industry experience to date indicates that for solid-free fluids values of $c = 100$ for continuous service and $c = 125$ for intermittent service are conservative", *i.e.* higher c-factors may be used. Although it is not clearly specified in API RP 14E, the solid-free condition mentioned in above statement is meant to cover corrosive fluids (*e.g.* production water) [31], so the resulting velocity limit actually refers to situations where FIC/FAC is an issue. "For solid-free fluids where corrosion is not anticipated or when corrosion is controlled by inhibition or by employing corrosion resistant alloys", API RP 14E recommends a higher c-factor of 150–200 for continuous service and up to 250 for intermittent service [25]. These three scenarios cannot be lumped together; when corrosion is not anticipated only mechanical erosion by liquid droplet impingement can occur, while when inhibition or corrosion resistant alloys (CRA) are employed erosion-corrosion might be a problem.

API RP 14E further instructs that "if solids production is anticipated, fluid velocities should be significantly reduced." However, it does not offer any specific guidance, even though this is the most critical scenario. Instead, API RP 14E suggests that appropriate c-factors need to be found from "specific application studies", *i.e.* through customized testing. Finally, API RP 14E recommends what seems to be an insurance policy that in conditions under which

Table 1
Recommended c-factors by API RP 14E for Eq. (1).

Fluid		Recommended c-factor	
		Continuous service	Intermittent service
Solids-free	Non-corrosive	150–200	250
	Corrosive + inhibitor	150–200	250
	Corrosive + CRA*	150–200	250
	Corrosive (?)	100	125
With solids		Determined from specific application studies	

* Corrosion resistant alloy.

solids are present, or corrosion is a concern or c-factors higher than 100 for continuous service are used –practically covering all imaginable scenarios– periodic surveys are required in order to assess pipe wall thickness [25]. In this statement, a mixture of erosion and erosion-corrosion scenarios is mentioned by API RP 14E, as if they are indistinguishable. Table 1 summarizes the c-factors suggested by API RP 14E for different conditions.

The API RP 14E erosional velocity equation (Eq. (1)) only needs the gas/liquid mixture density (ρ_m) in terms of input, which makes the equation easy to use. The following empirical equation is suggested by API RP 14E for calculating ρ_m:

$$\rho_m = \frac{12409 S_l P + 2.7 R S_g P}{198.7P + RTZ} \tag{2}$$

After calculating the erosional velocity (V_e), API RP 14E recommends using the equation below to determine "the minimum cross-sectional area required to avoid fluid erosion":

$$A = \frac{9.35 + \frac{ZRT}{21.25P}}{V_e} \tag{3}$$

While API RP 14E presents a simple equation to estimate the erosional velocity as a sizing criterion for pipework systems carrying two-phase gas/liquid flow, it is not clear at all how such a simple expression, with only one adjustable constant, can cover a broad array of scenarios seen in these systems; including various flow regimes (stratified, slug, annular-mist, bubble, churn, *etc.)*, the presence or absence of solids, the presence or absence of corrosion, with and without inhibition, and mild steel or CRA as the pipe material. The differences in erosion and erosion-corrosion mechanisms are so large that it seems next to impossible to capture all the possible scenarios with one such simple expression. However, before jumping to any conclusion, the origin of this empirical equation should be examined because it may form a rationale for its use.

3. Origin of API RP 14E erosional velocity equation

API RP 14E was first published in 1978. Ever since, its origin has been the subject of much debate in the open literature. The oldest reference found proposing an equation similar to the API RP 14E equation is Coulson and Richardson's Chemical Engineering book from 1979 [32]. It suggests the following empirical equation to obtain the velocity at which erosion becomes significant:

$$\rho_M u_M^2 = 15,000 \tag{4}$$

By solving Eq. (4) for the velocity (u_M) the same expression as the API RP 14 equation will be obtained with a c-factor of 122. When accounting for the conversion from SI units used in this reference to the Imperial units used in the API RP 14 equation, a c-factor of 100 is recovered. However, there is no information in the book about the origin of Eq. (4) either. It can be speculated that Eq. (4) represents some sort of an energy balance, with the left side representing the kinetic energy of the flow and the right side being the amount of energy required to cause erosion. A qualitatively similar argument was presented later by Lotz [33].

In 1983, Salama and Venkatesh [2] speculated that the API RP 14E equation might be not purely empirical and suggested three possible approaches that could theoretically justify its derivation. It is worth summarizing those arguments in an attempt to bring the reader closer to the origin of the API RP 14E equation:

(1) Bernoulli equation with a constant pressure drop
Solving the Bernoulli equation for velocity (V), assuming no gravity effects and a final velocity of zero results in Eq. (5), which has a similar form as the API RP 14E equation.

$$V = \frac{\sqrt{2\Delta P}}{\sqrt{\rho}} \tag{5}$$

Salama and Venkatesh [2] claimed that a typical total pressure drop for high capacity wells is between 3000 and 5000 psi. Substituting these numbers into Eq. (5) results in a c-factor in the range of 77–100. They concluded that although Eq. (5) and the API RP 14E equation seem to be similar, "they should have no correlation because they represent two completely different phenomena." [2] Indeed, it is difficult to imagine how the Bernoulli equation can be connected to erosion of a metal without introducing speculative assumptions along the way. One such hypothetical scenario would be flow of a fluid through a sudden constriction, such as the discharge of a valve or the suction of a pump, which causes an abrupt pressure drop that can be estimated by using (5). If the total pressure of the system falls below the vapor pressure of the liquid phase, cavitation could happen that leads to metal erosion [34–36]. Similar equations to Eq. (5) have been used to estimate the velocity limit above which cavitation erosion happens in pipeline systems [37–39].

(2) Erosion due to liquid impingement
In another attempt to justify the origin of the API RP 14E equation, Salama and Venkatesh [2] used the following equation introduced by Griffith and Rabinowicz for calculating the erosion rate due to liquid droplet impingement:

$$h = \frac{K\nu\rho V^2}{2Pg}\left(\frac{2}{27}\frac{\rho V^2}{gP\epsilon_c^2}\right)^2 \frac{1}{A} \tag{6}$$

By making a number of arbitrary assumptions, Salama and Venkatesh [2] were apparently able to reduce this equation to a form similar to the API RP 14E equation:

$$V \cong \frac{300}{\sqrt{\rho}} \tag{7}$$

For more details on the simplification procedure, the reader is referred to the original publication [2]. However, the authors of this paper determined that it was not possible to reproduce the derivation of Eq. (7) and recover the same c-factor (300). It seems that there was an inconsistency in the units in the original paper.

Craig [40] modified Salama and Venkatesh's simplifications of Eq. (6) using a high speed coefficient (K) of 10^{-5}, and units of ft/s for the penetration rate and psf for the target material hardness (P). Craig [40] proposed that liquid droplet impingement causes damage by removing the corrosion product layer from the surface and not removing the base metal itself as was originally considered by Salama and Venkatesh. Thus, in Eq. (6), Craig substituted the values of P and the critical failure strain (ϵ_c) for steel with those for magnetite (Fe_3O_4) ($P = 1.23 \times 10^8$ psf and $\epsilon_c = 0.003$). Craig's

simplification of Eq. (6) with a penetration rate of 10^{-11} ft/s resulted in the following equation:

$$V = \frac{150}{\sqrt{\rho^3}} \tag{8}$$

The denominators in Eqs. (7) and (8) are different, which proves the point made earlier about the inconsistency of units in the Salama and Venkatesh' calculations.

Using an argument similar to Craig, Smart [41] stated that the API RP 14E equation represents velocities needed to remove a corrosion product layer by "droplet impingement fatigue", as the flow regime in multiphase systems transits to annular mist flow (presumably an erosion-corrosion scenario). However, Arabnejad et al. [42] showed that the trend of the erosional velocity calculated by the API RP 14E equation did not correlate well with empirical data on erosion-corrosion caused by liquid droplet impingement. Deffenbaugh et al. [43] suggested that 400 ft/s is the approximate droplet impingement erosional velocity. The DNV GL recommended practice O501 suggests a threshold velocity of 230–262 ft/s to avoid droplet impingement erosion in gas-condensate systems [44]. If these velocities are plugged into the API RP 14E equation with a c-factor ranging from 100 to 300, the resulting mixture density falls between 0.06 and 1.7 lb/ft^3, which is extremely low for a gas/liquid two-phase flow mixture, making the linkage between the API RP 14E equation and liquid impingement implausible. Moreover, typical fluid velocities seen in oil and gas piping applications are far below the abovementioned droplet impingement erosional velocities, casting doubts that liquid droplet impingement can be considered as a reasonable erosional mechanism behind the API RP 14E equation [43].

(3) Removal of corrosion inhibitor films

As their last attempt, Salama and Venkatesh [2] assumed that the API RP 14E equation presents a velocity above which the flow could remove a protective corrosion inhibitor film from the surface of steel tubulars (an erosion-corrosion scenario). According to Salama and Venkatesh, the resulting erosional velocity can be calculated from the equation below:

$$V = \frac{\sqrt{\frac{8g\tau}{f}}}{\sqrt{\rho}} \tag{9}$$

Eq. (9) is apparently obtained by setting the flow-induced wall shear stress equal to the shear strength (τ) of the inhibitor film. However, Eq. (9) is not consistent when it comes to the units, *i.e.* the gravitational constant (g) does not fit into the equation [8,45]. Despite this, Salama and Venkatesh [2] derived an equation similar to the API RP 14E equation by simplifying Eq. (9) with τ equals 8000 psi and f equals 0.0015:

$$V = \frac{35,000}{\sqrt{\rho}} \tag{10}$$

Craig [40] reported that $f = 0.0015$ is meant for smooth pipes and $f = 0.03$ is more consistent with scale-roughened surfaces. In addition, Craig [40] used psf units instead of psi for τ in Eq. (9), resulting in a constant value of approximately 100,000 instead of 35,000 in Eq. (10). Either way, Eq. (10) has the same form as the API RP 14E equation; however, the constants found by Salama and Venkatesh as well as Craig were much larger than the c-factors proposed by API RP 14E, leading to very high velocities –orders of magnitude higher than those seen in the oil and gas industry. Therefore, even if the error in Eq. (10) is disregarded, it seems that the removal of the corrosion inhibitor film could not have been used as a background for deriving the API RP 14E equation.

In terms of a broader context for this argument, it should be noted that there is a longstanding belief, which is based on mostly anecdotal evidence, that above certain fluid velocities corrosion inhibition fails, what is often attributed to pure mechanical removal of the corrosion inhibitor film by the high wall shear stresses found in turbulent flow [36,46]. However, recent detailed studies have shown that pure mechanical removal of the inhibitor film from the metal surface by high-velocity flow is practically impossible, because the shear stresses required to remove a corrosion inhibitor film from the surface are of very high order (10^6–10^8 Pa), while the maximum wall shear stresses caused by highly turbulent multiphase flow in oil and gas fields are orders of magnitude lower (*ca.* 10^3 Pa) [36,47–49].

At the other end of the spectrum are authors who opined that the API RP 14E equation had no theoretical justification and that it is a purely empirical equation. A wide variety of sources was mentioned. For example, Smart [50] stated that the API RP 14E equation was apparently obtained from Keeth's report [51] on erosion-corrosion problems encountered in steam power plants, where multiphase steam condensate piping systems were used. However, no information on velocity limitation could be found in this report [31,51,52]. Castle et al. [53] claimed that the API RP 14E equation was formulated based on field experience with wells in the Gulf Coast area, as a criterion for the maximum velocity in carbon steel piping needed to avoid the removal of protective inhibitor films or corrosion products (an erosion-corrosion scenario). Heidersbach [54] suggested that the API RP 14E equation was adapted from a petroleum refinery practice in which the flow velocity was kept below the API RP 14E erosional velocity to minimize pumping requirements that become prohibitively expensive at high flow velocities. Salama [31] cited Gipson who mentioned that the proposed c-factor in the API RP 14E equation was meant to prevent excessive noise in piping systems. Wood [7] stated that the origin of the API RP 14E equation was from US Naval steam pipe specifications. Patton [55] reported that the API RP 14E equation was developed by the US Navy during World War II with a c-factor of 160 for carbon steel piping in solid-free fluids. Subsequently, the c-factor was changed to 100 when the equation was incorporated by the API. Another anecdote is that similar equations to the API RP 14E equation with c-factors ranging from 80 to 160 had been used in various oil companies before the API committee members wrote the API recommended practice 14E [50]; however, the origin of those equations was not specified.

Clearly, none of the abovementioned theoretical explanations (energy balance, Bernoulli equation, liquid impingement, corrosion inhibitor/product removal) that supposedly underpin the API RP 14E equation seem to properly justify its form. The alternative explanations involving anecdotal evidence are even less convincing. Subscribing to any of the above explanations about the origin of the API RP 14E does not change the fact that the API RP 14E equation has been used widely in the oil and gas industry, albeit with varying degrees of success. Therefore, it is worthwhile reviewing some of the publicized applications of the API RP 14E equation, followed by its misuses and limitations.

4. Some applications of API RP 14E erosional velocity equation

Although the origin and even the validity of the API RP 14E equation seems to be questionable, its application within the oil and gas industry has been prevalent. The following are a few examples of the application of the API RP 14E equation in the oil and gas industry.

Deffenbaugh and Buckingham [43] reported that Atlantic Richfield Company (ARCO) considered the API RP 14E equation as overly conservative for straight tubing with non-corrosive solid-free fluids. ARCO recommended a c-factor of 150 for continuous service and a c-factor of 250 for intermittent service when corrosion is prevented or controlled

by dehydrating the fluids, applying corrosion inhibitors or employing CRAs [43]. It is not entirely clear in this scenario how metal loss happened at all, when there were no solids in the flow stream, neither was there any corrosion.

Salama [24] has quoted Erichsen who reported data from a condensate field in the North Sea operating with a *c*-factor of 726 (equivalent to a flow velocity of 286 ft/s) for 3 years until a failure occurred in AISI 4140 carbon steel tubing at the flow coupling, which was attributed to liquid droplet impingement. Another operator in the North Sea chose a *c*-factor of 300 as the upper limit for the Gullfaks oil field subsea water injectors completed with API L80 13Cr tubing.

Chevron produced from a gas-condensate reservoir in the North West Shelf of Western Australia with a pressure of 4500 psi and temperature of 110 °C at a velocity just below the wellhead of 121 ft/s (corresponding to a *c*-factor of 400) in 7″ OD tubing and at 59 ft/s (corresponding to a *c*-factor of 200) in 9 5/8″ OD tubing with no failure [56].

At North Rankin offshore gas field in the North West region of Western Australia, velocities up to 98 ft/s, three times the API recommended erosional velocity, were handled in carbon steel tubing over long periods of production without any sign of erosion [53].

In a field study done by the National Iranian Oil Company on four gas wells in the Parsian gas-condensate field in southern Iran, *c*-factors in the range of 149 (velocity of 55 ft/s) to 195 (velocity of 74 ft/s) caused no unexpected erosion damage. Therefore, the operator suggested using an average *c*-factor of 170 as a safe value for all those wells [27]. In similar research conducted on four gas-condensate wells in the South Pars gas field in southern Iran, it was reported that *c*-factors in the range of 138–193 were safe for production [57].

BP Amoco limited the velocities in production from gas wells in the Endicott field of the Alaskan North Slope to approximately three times the API erosional velocity based on an experience that fluids with very small amounts of entrained solids flowing through SS pipelines caused minimal risk of erosion at those velocities [58].

Before 1993, Shell used a modified version of the API RP 14E equation with a *c*-factor of 160 for sand-free, 120 for moderate-sand and 80 for severe-sand service. Since 1993 and before switching to a modified version of the Tulsa Model (see Section 7.5), Shell stopped using the API RP 14E equation and set the limiting erosional velocity directly according to the type of failure mechanism, and verified that velocity with appropriate monitoring and inspection [59].

TOTAL has been using the API RP 14E equation to define erosion-corrosion velocity limits for carbon steel facilities, sometimes in combination with fixed velocities not to be exceeded, whichever is smaller. For CRAs, copper alloys, and nonmetallic materials fixed velocity limits are solely used. TOTAL has specific criteria (decision tables) in case of erosion-corrosion for determining the most appropriate *c*-factor ranging from 75 to 250 based on the concentration of solid particles, the main produced phases (liquid or multiphase, gas dominant or oil dominant), the corrosiveness of the water (if any), and the presence of corrosion inhibitors. Below is a summary of the decision tables:

- *c*-factors < 100 for corrosive fluids containing significant amounts of solid particles, which are considered highly detrimental in terms of erosion-corrosion;
- *c*-factors from 100 to 160 for various liquid or multiphase fluids, depending on their corrosiveness and the confidence given to the corrosion mitigation;
- *c*-factors from 200 to 300 for fluids not significantly corrosive and without significant amount of solid particles (*e.g.* deaerated seawater, dry gas, *etc.)* [60].

TOTAL apparently does not use the API RP 14E equation to determine the erosional velocity when pure mechanical erosion is involved. TOTAL defines an indicative velocity limit of 50 m/s for passivating alloys such as stainless steel (SS) as a typical “hold point” above which pure erosion might happen in the presence of trace amounts of solid particles. This 50 m/s value is not a definitive velocity limit but rather a break point for further assessment of the conditions. Generally, TOTAL uses specially developed erosion models such as the DNV GL model (Section 7.4) or the Tulsa model (Section 7.5) for predicting pure erosional damages [60].

It is quite possible that the above practices no longer reflect the current practices being used in the mentioned companies. Even then, in almost all the reported field cases, *c*-factors higher than those suggested by API RP 14E were used, with a very large spread.

5. Misuses of API RP 14E erosional velocity equation

The API RP 14E equation was intended for establishing an erosional velocity in “new piping systems on production platforms located offshore”, transporting gas and liquid two-phase fluids. API RP 14E clearly states a specific range of *c*-factors for “solid-free fluids where corrosion is not anticipated or when corrosion is controlled by inhibition or by employing CRAs”. These conditions are commonly recognized as “clean” service. Presumably, for solid-free corrosive fluids the API RP 14E equation can also be used with a *c*-factor of 100, although it is considered conservative. In the presence of solids, reduced *c*-factors are recommended if “specific application studies have shown them to be appropriate”, without an explicit guideline provided by the API RP 14E [25]. Obviously, in conditions other than those mentioned above, the API RP 14E equation should not be used, at least not without a proper justification.

Probably due to a lack of alternatives and its simplicity, the API RP 14E equation has been used widely with arbitrary choice of *c*-factors for a variety of unfitting conditions such as single-phase flow service and uninhibited corrosive systems with a corrosion product layer [24,52,61]. Another problematic use of the API RP 14E equation was for sizing downhole tubulars, which were not included in the original recommended practice [23,50,54]. The steel grade recommended for downhole tubulars (specified in API SPEC 5CT [62]) is generally stronger and harder than API 5 L steel grade recommended in API RP 14E [54]. Therefore, if applicable at all, the original API RP 14E erosional velocity would be conservative for downhole tubulars.

The lack of generality of the API RP 14E equation was clearly recognized in the past, and some attempts were made to improve its performance by presenting functions for calculation of the *c*-factor at different operating conditions [31]. However, this just compounded the problem where an empirical equation–which already performed inadequately and could not be extrapolated across different conditions–was altered by making it even more complex, without proper justifications.

In the most general sense, the misuse of the API RP 14E equation stems from its doubtful origin and unclear theoretical basis, what led to it being used in all kinds of conditions and applications for which it was not intended. This is based on a problematic assumption (often implicit) that the API RP 14E equation can be used as a means of generalizing observed empirical erosion, FIC/FAC or erosion-corrosion data to derive safe operational velocities for a broad variety of conditions, usually outside operational or experimental ranges. This assumption ignores the fact that the mechanism and the rate of degradation can be very different (by orders of magnitude) depending on type of service or even within the same type of service. Therefore, the API RP 14E equation cannot be simply applied to all kinds of conditions by just modifying the *c*-factor, assuming that the equation is universally valid and it will give reasonable values.

The dubious origin and the unfavorable assessment of the validity of the API RP 14E equation cannot be ignored, boldly assuming that it is correct and can be used unquestionably (obviously done so many times before); one should be aware of its serious limitations, which are summarized in the following section.

6. Limitations of API RP 14E erosional velocity equation

The API RP 14E equation while offering a simple approach to calculate the erosional velocity, has some serious limitations:

- The equation only considers the density of fluid in calculating the erosional velocity, while many other influential factors such as pipe material, fluid properties, flow geometry and flow regime are not accounted [23,63,64].
- The API RP 14E equation treats flow lines, production manifolds, process headers and other lines transporting oil and gas similarly in terms of limiting the velocity. However, areas with flow disturbances such as chokes, elbows, long radius bends, and tees, where most of the erosion/corrosion problems occur, are not differentiated by the API RP 14E equation [63,65].
- The API RP 14E equation suggests that the limiting erosional velocity increases when the fluid density decreases. This does not agree with experimental observations for sand erosion and liquid droplet impingement in which erosion is higher in low-density fluids [2,23]. In high-density fluids most solid particles are carried in the center of the flow stream without significantly impacting the surface [2]. Moreover, the presence of a high-density fluid cushions the impact of solid particles or droplets at the pipe wall. Thus, a higher limiting erosional velocity can actually be applied to fluids with a higher density [21].
- The API RP 14E equation does not offer any guidelines regarding how to estimate the erosion rate, neither below nor above the limiting erosional velocity. It also does not specify a general allowable erosion rate, in terms of rate of wall thickness loss (*e.g.* 5–10 mpy) [23].
- Probably the most significant limitation of the API RP 14E equation is that it does not provide any quantitative guidelines for estimating the erosional velocity when solids are present in the production fluid (erosion) or when erosion and corrosion are both an issue (erosion-corrosion), assuming that $c = 100$ is defined for corrosion service. Some amount of solid particles as well as a certain degree of corrosion are almost inevitable in real production systems [43,50]. Even in so-called “sand-free” or “clean” service, where sand production rates are as low as a few lb/day, erosion and erosion-corrosion damage could be very severe at high production velocities [23]. Therefore, in most of the alternatives to the API RP 14E equation (described below), the effect of erosion by sand particles is the focus. However, the effects of flow on mixed erosion-corrosion scenarios have not been properly addressed in the open literature due to the complexity of erosion-corrosion process. Over the past decade an approach called erosion-corrosion mapping sometimes in combination with computational fluid dynamics (CFD) has been employed in modeling of erosion-corrosion [66]. Erosion-corrosion mapping identifies the relative contributions of erosion, corrosion (whether it is active dissolution or passivation), flow and their synergistic effects on the total wastage rate [67]. For review of recent advances in the area of predictive models for erosion-corrosion, the reader is directed to Refs. [66–68].

7. Alternatives to API RP 14E erosional velocity equation

Given the problematic origin of the API RP 14E erosional velocity equation, its misuses and limitations, it is worthwhile to take a look at some key alternatives that are available in the open literature.

When it comes to the intent and scope, some of these alternatives discussed below overlap largely with API RP 14E, and in some aspects go beyond the narrow application range of the API RP 14E erosional velocity equation. Examples are the NORSOK P-002 standard [68] and to some extent the recommendations of Svedeman and Arnold [63].

In other cases, the alternatives focus on addressing one of the most important limitations of the API RP 14E equation –how to derive velocity limits in the presence of solid particles, beyond just arbitrarily using the API RP 14E erosional velocity equation with a smaller c-factor. These alternatives are usually based on field experience, empirical correlations or theoretical models. Most theoretical models evaluate erosion based on the displaced volume of metal or dissipation of energy during particle impact on the metal surface [69]. The best-known examples of such sand erosion models that have been commonly used in the oil and gas industry are the Salama model, the DNV GL model and the various versions of the Tulsa model. In the following sections, these alternatives are reviewed and compared with each other, whenever possible.

7.1. NORSOK P-002 standard

The NORSOK P-002 standard [68] was developed by the Norwegian petroleum industry to provide “requirements for the following aspects of topside process piping and equipment design on offshore production facilities: design pressure and temperature; safety instrumented secondary pressure protection systems; line sizing; system and equipment isolation; and insulation and heat tracing.” NORSOK P-002 defines standard criteria for sizing pipes in new installations, mainly based on pressure drop and erosional velocity, similarly as is done in API RP 14E. Actually, the NORSOK P-002 standard recommends that sizing lines in general should be in accordance with ISO 13703 [70], which is based on API RP 14E. Just like API RP 14E, the NORSOK P-002 standard divides the flow lines into three main categories: single-phase gas, single-phase liquid and two-phase/multiphase gas/liquid lines [68]. The erosional velocity limits for each category are briefly discussed below:

1. Single-phase gas lines
   For single-phase gas lines where pressure drop is not critical, the standard requires not to exceed velocities, which may create noise or vibration problems. As a rule-of-thumb, the standard suggests keeping the velocity below the following equation or 60 m/s, whichever is lower, to avoid noise problem:

   $$V = 175 \times (1/\rho)^{0.43} \quad (11)$$

   The constant 175 may be replaced with 200 during process upsets, if the noise level is acceptable. Although Eq. (11) is for avoiding noise, it is similar in form to the API RP 14E equation. The standard states that if solid particles exist in the gas, particle erosion and an allowable erosion rate should be considered for determination of the maximum velocity, without being any more specific about it [68].
2. Single-phase liquid lines
   For single-phase liquid lines, the standard advises to keep the velocity sufficiently low to prevent problems with erosion, water-hammer pressure surges, noise, vibration, and reaction forces. Table 2 summarizes the recommended maximum velocities for different conditions and materials in continuous service, although is not clear how these limits were derived and what was the limiting Criterion. For intermittent service, the NORSOK P-002 standard allows using a maximum velocity of 10 m/s depending on the duration and frequency of operation [68].
3. Two-phase and multiphase gas/liquid lines
   The NORSOK P-002 standard states that: “Wellhead flow-lines, production manifolds, process headers and other lines made of steel and transporting two-phase or multiphase flow, have a velocity limitation. When determining the maximum allowable velocity, factors such as piping geometry, well-stream composition, sand particle (or proppant) contamination and the material choice for the line shall be considered.” Then the standard recommends the following equation to calculate the maximum velocity:

   $$V = 183 \times (1/\rho_m)^{0.5} \quad (12)$$

Table 2
Recommended maximum velocities for liquid lines according to NORSOK P-002 [68].

Fluid	Maximum velocity (m/s)			
	CS	SS/Titanium	CuNi[c]	GRP
Liquids	6	7[b]	3	6
Liquids with sand[d]	5	7	n/a	6
Liquids with large quantities of mud or silt[d]	4	4	n/a	n/a
Untreated seawater[a]	3	7	3	6
Deoxygenated seawater	6	7[b]	3	6

CS: carbon steel; SS: stainless steel; GRP: glass fiber-reinforced plastic.
[a] For pipe diameters less than 8 in (DN 200), BS MA-18 standard [71] is suggested.
[b] For SS and titanium the maximum velocity is limited by system design (available pressure drop/reaction forces). 7 m/s may be used as a typical starting value for sizing.
[c] Minimum velocity for CuNi is 1 m/s.
[d] Minimum velocity for liquids with sand should be in accordance with ISO 13703 [70].

NORSOK P-002 does neither indicate the source nor the reasoning behind Eq. (12), even if it is obvious that in form it is identical to the API RP 14E erosional velocity equation. When adjusting for the units, the constant in Eq. (12) matches with the *c*-factor of 150 recommended by API RP 14E.

For non-corrosive well streams and for corrosion resistant pipe materials, with small amounts of solid particles (typically less than 30 mg sand/liter in the mixed flow) the NORSOK P-002 standard limits the maximum velocity to 25 m/s. For well streams with larger amounts of solids, the NORSOK P-002 standard suggests calculating the maximum allowable velocity based on "sand concentration, piping geometry (bend radius, restrictions), pipe size, and added erosion allowance." For this, one presumably needs to use erosion models such as those described below; however, no more specific guidance is provided [68].

For corrosive service (apparently in case of FIC/FAC and erosion-corrosion) where carbon steel piping is used, the NORSOK P-002 standard recommends restricting the maximum velocity to 10 m/s to avoid removal of the protective corrosion product layer and/or corrosion inhibitor films, although the rationale behind this limiting velocity is not mentioned [68].

Comparing the velocity limits given by the NORSOK P-002 standard with those estimated by the API RP 14E equation at similar conditions shows that the NORSOK P-002 standard is less conservative than the API RP 14E equation.

7.2. Svedeman and Arnold

Svedeman and Arnold [63] recommended using the following criteria for determining the erosional velocity in "flow lines, production manifolds, process headers, and other lines transporting gas and liquid two-phase flow":

(1) For clean service
Clean service was defined as sand-free non-corrosive fluids (absence of corrosive species or application of corrosion resistant alloys or corrosion inhibitors), where liquid-droplet impingement is the only possible cause of erosion of the base metal. Based on various laboratory studies, Svedeman and Arnold suggested that no erosion occurs up to at least 100 ft/s (possibly even up to 300 ft/s) for the clean service.
(2) For erosive service
For erosive service involving solid particles, Svedeman and Arnold [63] adopted the following equation for predicting the erosional velocity in pipe fittings based on Bourgoyne's empirical approach [72]:

$$V_e = K_s \frac{d}{\sqrt{q_s}} \tag{13}$$

Eq. (13) was derived based on an allowable metal erosion rate of 5 mpy. The values of the fitting erosion constant (K_s) for different component geometries, materials and flow regimes can be found in Ref. [73].
(3) For corrosive service
According to Svedeman and Arnold, in corrosive service, the erosion criterion is removal of the corrosion product layer from the surface due to liquid droplet impingement, which occurs when the flow regime is annular-mist. Therefore, the velocity should be kept below the transition velocity for the annular-mist flow regime. However, it is mentioned that further experimental work is needed to prove the appropriateness of this approach.
(4) For erosive-corrosive service
For erosive-corrosive service, the mechanism of material loss is the combined effect of erosion and corrosion. No velocity limit is proposed in this case because the interaction of erosion and corrosion is complicated. This case was left open for further investigations [63].

7.3. Salama model

Salama [24] proposed the following criteria for estimating the erosional velocity in multiphase flow:

(1) For solid-free, non-corrosive fluids when pressure drop is not a concern, the API RP 14E equation with a *c*-factor of 400 is recommended (apparently covering liquid droplet impingement).
(2) For solid-free, corrosive fluids, the API RP 14E equation with *c*-factors higher than 300 can be used, provided that the inhibitors being used in the system remain effective at velocities corresponding to these *c*-factors (clearly referring to an FIC/FAC scenario).
(3) For sand-laden fluids, the erosional velocity can be calculated from Eq. (14) by considering an allowable erosion rate for the system, for example 0.1 mm/y.

$$ER = \frac{1}{S_m} \frac{W V_m^2 d}{D^2 \rho_m} \tag{14}$$

Eq. (14) is a semi-empirical equation for predicting erosion caused by sand-laden multiphase fluids in pipe bends [24]. Salama suggested a value of 5.5 for the geometry-dependent constant (S_m) for pipe bends based on experimental results. The effect of bend radius was not considered in the Salama model because test results did not show a major difference in the erosion rates for 1.5 and 5*D* bends [24].

7.4. DNV GL-RP-O501

DNV GL-RP-O501 is a guideline on "how to safely and cost effectively manage the consequences of sand produced from the oil and gas reservoirs through production wells, flowlines and processing facilities." [44] Major oil and gas operators such as Statoil, Norsk Hydro, ConocoPhillips, and Amoco have contributed to the development of this guideline [74]. DNV GL-RP-O501 qualitatively ranks the erosion potential for piping systems with reference to bulk flow velocities, considering the flow velocity as the only parameter that affects erosion (Table 2-1 of the original standard). DNV GL-RP-O501 suggests the following general empirical equation for quantitative assessment of sand particle erosion [44]:

$$E_m = K \cdot U_p^n \cdot F(\alpha) \cdot m_p \tag{15}$$

For CS, duplex SS, 316 SS, and Inconel (Ni-Cr alloy), the material coefficients (K) and the velocity exponent (n) are 2×10^{-9} and 2.6, respectively. For other materials, the reader is referred to Table 3-1 of the original standard. The particle impact velocity (U_P) is assumed to be equal to the mixture flow velocity (V_m), which is the summation of superficial velocities of all phases. The impact angle function ($F(\alpha)$) describes the dependency of erosion on the particle impact angle. For ductile materials including steel grades, $F(\alpha)$ can be calculated from the following equation [44]:

$$F(\alpha) = 0.6[\sin(\alpha) + 7.2(\sin(\alpha) - sin^2(\alpha))]^{0.6} \bullet [1 - \exp(-20\alpha)]$$
$$F(\alpha) \in [0,\ 1] \text{ for } \alpha \in \left[0, \frac{\pi}{2}\right] \tag{16}$$

Eq. (15) is the general correlation for erosion rate prediction developed empirically by Finnie in 1960 [75]. DNV GL-RP-O501 suggests corrections to Eq. (15) for different piping components (*e.g.* straight pipes, elbows, blinded tees, welded joints, and reducers), accounting for parameters such as size, concentration, and multiple impact of sand particles; the geometry of components; and the distance of straight piping between the components. These corrections were determined by detailed CFD erosion simulations and by comparison of model results with field experience [44].

For smooth and straight pipes under turbulent conditions, the suggested equation is as follows:

$$E_L = 2.5 \times 10^{-5} U_P^{2.6} \bullet\ m_p\ \bullet\ D^{-2} \tag{17}$$

It should be noted that Eq. (17) is independent of the fluid density, viscosity, and particle size.

For disturbed flow geometries, different procedures are suggested to calculate the erosion rate. As an example, below is the procedure for predicting the erosion rate in bends [44]:

(1) Calculate the characteristic impact angle (α):

$$\alpha = \arctan\left(\frac{1}{\sqrt{2 \bullet R}}\right) \tag{18}$$

For a 5D bend, R and α are equal to 5 and 0.3, respectively.

(2) Compute the dimensionless parameters A and β:

$$A = \frac{\rho_m^2 \bullet \tan(\alpha) \bullet U_P \bullet D}{\rho_P \bullet \mu_m} \tag{19}$$

$$\beta = \frac{\rho_P}{\rho_m} \tag{20}$$

(3) Calculate the ratio (γ) and the critical ratio (γ_c) of particle diameter (d_P) to geometrical diameter (D) using the parameters obtained in step 2:

$$\frac{d_{P,c}}{D} = \gamma_c = \begin{cases} \frac{1}{\beta[1.88\ln(A) - 6.04]} & 0 < \gamma_c < 0.1 \\ 0.1 & \gamma_c \le 0 \text{ or } \gamma_c \ge 0.1 \end{cases} \tag{21}$$

$$\gamma = \frac{d_P}{D} \tag{22}$$

(4) Determine the particle-size correction function (G) by using the parameters found in step 3:

$$G = \begin{cases} \frac{\gamma}{\gamma_c} & \gamma < \gamma_c \\ 1 & \gamma \ge \gamma_c \end{cases} \tag{23}$$

(5) Calculate the characteristic pipe bend area exposed to erosion:

$$A_t = \frac{\pi D^2}{4\sin(\alpha)} = \frac{A_{pipe}}{\sin(\alpha)} \tag{24}$$

(6) Determine the value of the impact angle function from Eq. (16) by using the angle found in Step 1.

(7) The model/geometry factor (C_1) is set equal to:

$$C_1 = 2.5 \tag{25}$$

C_1 accounts for multiple impact of the sand particles, concentration of particles at the outer part of the bend and model uncertainty.

(8) For m/s to mm/y conversion, the following unit conversion factor must be used:

$$C_{unit} = 1000 \bullet 3600 \bullet 24 \bullet 365 = 3.15 \times 10^{10} \tag{26}$$

(9) The maximum erosion rate (mm/y) in a pipe bend is estimated by using the following expression:

$$E_{L,y} = \frac{K \bullet F(\alpha).\ U_P^n}{\rho_t \bullet A_t} \bullet G \bullet C_1 \bullet GF \bullet m_P \bullet C_{unit} \tag{27}$$

The geometry factor (GF) is considered to be 1 based on an assumption that the straight pipe section upstream the bend is greater than 10D. When the distance of straight piping is less than 10D, a different GF should be used. For more details about GF and other type of flow geometries, the reader is referred to the original standard. DNV GL-RP-O501 suggests that for each specific system design and operating conditions, further CFD erosion simulations and/or experimental investigations might be needed to estimate the erosion rate accurately [44].

For an allowable erosion rate (*e.g.* 0.1 mm/y), the erosional velocity can be calculated by solving Eq. (27) for U_P. The empirical models suggested by DNVGL-RP-O501 only address erosion by solids and do not account for erosion-corrosion, or other mechanisms such as droplet impingement erosion or cavitation. The models are applicable only where quartz sand is the erosive agent. Moreover, there are limitations to the range of model input parameters, found in Table 4-1 of the original standard [44]. The DNV GL model is applicable to all multiphase flow regimes [76]. An engineering software called Pipeng Toolbox (pipeng.com) has been developed based on DNV GL-RP-O501 that enables a simple and time efficient assessment of sand erosion potential for standard piping components.

7.5. Tulsa model

The Tulsa model refers to a series of semi-empirical models developed by the Erosion/Corrosion Research Center (E/CRC) at The University of Tulsa for estimating erosion rate and safe operating velocity in oil and gas flow lines where sand is present [77,78]. The Tulsa model is currently the most widely used tool for sand erosion assessment in major oil and gas companies. The original model was developed in 1993 for single-phase flow; however, over time it was extended to cover multiphase flow conditions [23,79,80]. Eq. (28) is one of the early versions of the Tulsa model that allows the calculation of the maximum erosion rate in elbows for both single and multiphase flow [80]:

$$h = F_M F_s F_P F_{r/D} \frac{W}{\left(\frac{D}{D_o}\right)^2} V_L^{1.73} \tag{28}$$

The pipe diameter (D) and the sand production rate (W) are assumed to be known. The material hardness coefficient (F_M) that accounts for the effect of target (pipe) material on erosion is obtained

Table 3
The values for B and C in Eq. (29) [59,79].

Material	Brinell hardness (B)	C	
		for V_L in m/s	for V_L in ft/s
AISI 1018	210	1.95E-05	2.50E-06
AISI 1020	150	1.94E-05	2.49E-06
13Cr annealed	190	2.80E-05	3.59E-06
13Cr heat treated	180	2.33E-05	2.98E-06
2205 duplex	217	1.88E-05	2.41E-06
316 SS	183	1.98E-05	2.54E-06
API Q125	290	1.95E-05	2.50E-06
Incoloy 825	160	1.75E-05	2.24E-06

using the following equation [77]:

$$F_M = C \cdot B^{-0.59} \tag{29}$$

Table 3 lists the values of Brinell hardness (B) and empirical constant (C) for different pipe materials.

The particle shape coefficient (F_s) is an empirical parameter used to account for the effect of particle shape on erosion. Table 4 shows the values of F_s for different particle shapes.

The penetration factor (F_P) was defined as the decrease in the thickness of the eroded material per unit of mass loss of that same material. It can be seen as a measure of how concentrated the erosion attack is, depending on the geometry of the component. F_P was established for a reference pipe with 1-in ID (D_o = 1 in). The term $(D/D_o)^2$ in Eq. (28) was used to correct F_p for the pipe diameter [79]. Table 5 shows the F_p values for different geometries.

The penetration factor for elbow radius ($F_{r/D}$) is a semi-empirical parameter developed to take into account the effect of elbow geometry and particle size on erosion. The following equation was suggested to calculate $F_{r/D}$ for a particle density of approximately 165 lb/ft^3 (2650 kg/m^3) [80]:

$$F_{r/D} = \exp\left(-\left(0.1\frac{\rho_f^{0.4}\mu_f^{0.65}}{d_p^{0.3}}+0.015\rho_f^{0.25}+0.12\right)\left(\frac{r}{D}-C_{std}\right)\right) \tag{30}$$

For pipe geometries other than the elbow, $F_{r/D}$ was presumably considered to be 1.

The characteristic particle impact velocity (V_L) in Eq. (28) is the particle velocity when the particle hits the pipe wall [82]. In order to calculate V_L in a complex pipe geometry such as a tee or an elbow, the erosion in that geometry was related to the erosion occurring in a simple 90° impingement situation [23,77,78]. Sand particles, before impinging the pipe wall and causing erosion, enter a region near the wall in which their motion will be retarded by the fluid. This region is called the stagnation zone and its length is called the stagnation length [78,82]. Fig. 1 illustrates graphically the concepts of the stagnation zone and the stagnation length.

For a given pipe geometry, an equivalent stagnation length (L) was defined with reference to the stagnation length of a simple 90° impingement situation that will result in the same erosion rate as the average erosion rate in that geometry. L was determined by conducting erosion experiments for small pipe diameters followed by extrapolating the data to larger pipe diameters, using CFD simulations. For elbows and tees, L can be calculated using the following semi-empirical equations, respectively [79]:

$$\frac{L}{L_o} = 1 - 1.27tan^{-1}(1.01D^{-1.89}) + D^{0.129}$$
$$L_o = 1.18\ in \tag{31}$$

$$\frac{L}{L_o} = 1.35 - 1.32tan^{-1}(1.63D^{-2.96}) + D^{0.247}$$
$$L_o = 1.06\ in \tag{32}$$

Table 4
The particle shape coefficient (F_s) in Eq. (28) [23].

Particle shape	F_s
Sharp corners (angular)	1.00
Semi-rounded (rounded corners)	0.53
Fully rounded	0.20

Table 5
The penetration factor (F_P) in Eq. (28) [59,81].

Geometry	F_P (for CS)		F_P (for SS316)	
	m/kg	in/lb	m/kg	in/lb
90° elbow	0.206	3.68	0.631	11.26
Tee	0.206	3.68	n/a	n/a
Choke	0.055	0.98	n/a	n/a
Direct impingement	0.224	4.00	n/a	n/a

Eqs. (31) and (32) are not applicable for diameters smaller than 1″ [80].

A simplified particle tracking model was suggested to compute the particle velocity profile along the stagnation zone (V_P), assuming that when a particle enters the stagnation zone it travels through a 1D-flow field and only a drag force acts on the particle [23,77]:

$$\frac{dV_P}{dx} = 0.75\left(\frac{1}{d_P}\right)\left(\frac{\rho_f}{\rho_P}\right)\left[\frac{0.5(V_f - V_P)|V_f - V_p|}{V_P} + \frac{24\mu_f(V_f - V_P)}{V_P\rho_f d_P}\right] \tag{33}$$

V_f in Eq. (33) is the fluid velocity along the stagnation zone, which was assumed to decrease linearly from the fluid bulk (average) velocity (V_o) at the beginning of the stagnation zone (x = 0) to zero at the target wall (x = L) (See Fig. 1) [82]:

$$V_f = V_o\left(1-\frac{x}{L}\right) \tag{34}$$

Generally, V_p is not the same as V_f [82].

V_L is equal to V_P at the pipe wall (x = $L - \frac{d_P}{2}$) and can be determined by solving Eq. (33) with a boundary condition of $V_P = V_o$ at $x = 0$. Finally, the penetration rate (h) can be determined by substituting all the parameters explained above into Eq. (28).

In 2005, Oka et al. [83,84] proposed a new version of the Tulsa model by assuming that erosion damage at an arbitrary impact angle ($E(\alpha)$) is equal to the erosion damage at normal impact angle (E_{90}) multiplied by a function ($g(\alpha)$) that accounts for the effect of impact angle on the erosion damage. They expressed the erosion predictive equation in terms of unit of material volume loss per mass of particles (mm^3/kg) as follows:

$$E(\alpha) = g(\alpha)E_{90} \tag{35}$$

$$E_{90} = K(H_V)^{k_1}\left(\frac{V_P}{V'}\right)^{k_2}\left(\frac{D_P}{D'}\right)^{k_3} \tag{36}$$

$$g(\alpha) = (\sin\alpha)^{n1}(1+H_V(1-\sin\alpha))^{n_2} \tag{37}$$

$$n_1 = s_1(H_V)^{q_1},\ n_2 = s_2(H_V)^{q_2} \tag{38}$$

All parameters in the Oka et al. [83,84] model were obtained empirically. Table 6 shows the values of these parameters for a type of sand (density = 2600 kg/m^3) typically found in oil and gas fields.

Zhang et al. [85] in 2007 proposed a modified version of the Tulsa model as presented below:

$$ER = CB^{-0.59}F_s V_L^{2.41}F(\theta) \tag{39}$$

The erosion ratio (ER) in Eq. (39) was defined as the ratio of target mass loss to the total mass of particles impacting the target. The erosion ratio can be converted to the penetration rate (h) by using the following

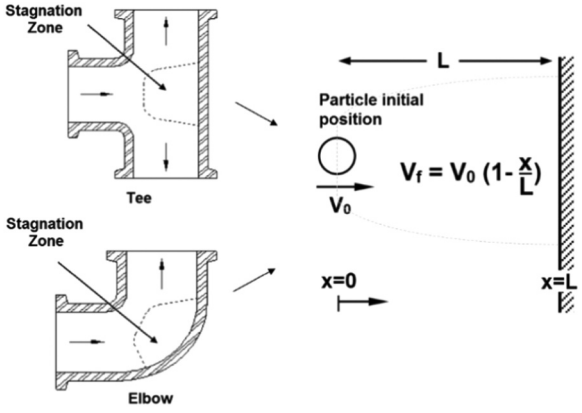

Fig. 1. Graphical illustration of the stagnation zone and the stagnation length. Adopted from Ref. [80]. V_o is the fluid bulk (average) velocity; V_f is the fluid velocity along the stagnation zone; L is the equivalent stagnation length or the length of the stagnation zone in a direct 90° impingement geometry; and x is the particle location along the stagnation zone.

equation:

$$h = ER\frac{F_P W}{(D/D_o)^2} \tag{40}$$

The material's Brinell hardness in Eq. (39) was related to the Vicker's hardness by the equation below:

$$B = \frac{H_V + 0.1023}{0.0108} \tag{41}$$

For the impact angle function ($F(\theta)$) in Eq. (39) a polynomial function was proposed by Zhang et al. [85] as follows:

$$F(\theta) = \sum_{i=0}^{5} A_i \theta^i \tag{42}$$

The values for empirical coefficients (A_i) and the corresponding C constant in Eq. (39) are given Table 7.

$F(\theta)$ depends on the target material, particle properties and flow conditions. $F(\theta)$ varies between zero and one. For ductile materials such as steels, different values have been reported for the impact angle (θ) at which the maximum erosion occurs, ranging from 15° to 60° [24,69,75,76,85,87].

In 2009, Torabzadehkhorasani [88] and Okita [89] suggested a new version of $F(\theta)$ based on the Oka et al. model (Eq. (37)):

$$F(\theta) = \frac{1}{f}(sin\theta)^{n_1}(1+H_V^{n_3}(1-sin\theta))^{n_2} \tag{43}$$

Table 8 summarizes f and n_i in Eq. (43) and the corresponding C constant in Eq. (39) for different target materials and test conditions. The reader is encouraged to check the experimental details for each case listed in Table 8 in order to establish a relevance for their case.

There are other versions of the Tulsa model that came after Eq. (39), such as Arabnejad et al. [69] and Shirazi et al. [95] versions. However, the most popular version of the Tulsa model at present is Eq. (39).

The early (Eq. (28)) and the new (Eq. (39)) versions of the Tulsa model have the same form (see Eq. (40)) except for the impact angle function and the velocity exponent. The term $F_{r/D}$ in the early version seems to be substituted with $F(\theta)$ in the new version. Both terms account for pipe geometry in erosion calculations. Moreover, it can be guessed that $F(\theta)$ in the early version of the Tulsa model was considered to be 1, in order to give the maximum penetration rate.

When it comes to the velocity exponent in the Tulsa model, Zhang [96] observed that 1.73 over-predicted the erosion rate and suggested to use 2.41 (along with a smaller C constant), instead. However, in certain cases acceptable results have been obtained by using 1.73 [81]. The velocity exponent is an empirical value that varies with change in the target material, particle properties and flow conditions. Vieira [81] reported velocity exponents of 2.71 and 2.77 for SS 316 in single-phase air flow with 150 and 300 μm sand particles, respectively; or 2.93 for Inconel 625 in the same flow with 300 μm sand particles. In another research, Vieira et al. [87] reported velocity exponents of 2.39 for 300 μm and 2.49 for 150 μm sand particles in single-phase air flow. Mansouri [93] showed that in dry impact testing with single-phase air flow, 300 μm sand size and SS 316 target material, the velocity exponent varied from 2.45 for 15° to 2.58 for 90° impact angle. However, 2.41 was chosen as the velocity exponent for all pipe materials, sand particles, and flow conditions in Eq. (39) and the C constant was changed alternatively. The values for the C constant shown in Table 8 are calculated by taking the average of the experimental results at a specific test condition [93].

In the Tulsa model, it is suggested that for multiphase flow, the fluid mixture properties should be used wherever applicable. Mixture properties such as mixture density and viscosity can be obtained from the following equations:

$$\rho_m = \frac{V_{SL}}{V_{SL}+V_{SG}}\rho_L + \frac{V_{SG}}{V_{SL}+V_{SG}}\rho_G \tag{44}$$

$$\mu_m = \frac{V_{SL}}{V_{SL}+V_{SG}}\mu_L + \frac{V_{SG}}{V_{SL}+V_{SG}}\mu_G \tag{45}$$

The mixture velocity (V_m) in the API RP 14E equation and all the alternative models discussed in this article was assumed to be equal to the average fluid velocity (V_o) and expressed as the summation of superficial liquid (V_{SL}) and superficial gas (V_{SG}) velocities [24,25,73,97]:

$$V_m = V_o = V_{SG} + V_{SL} \tag{46}$$

However, alternatively, a set of *ad-hoc* equations was also proposed for the Tulsa model to calculate V_o in terms of V_{SL} and V_{SG} [97]:

$$V_o = \lambda_L^n V_{SL} + |1-\lambda_L|^n V_{SG} \tag{47}$$

Table 6
Empirical constants and exponents in Eqs. (36)–(38) [83,84].

Particle	K	k_1	k_2	k_3	s_1	q_1	s_2	q_2	V' (m/s)	D' (μm)
SiO_2-1	65	−0.12	$2.3(H_v)^{0.038}$	0.19	0.71	0.14	2.4	−0.94	104	326

Table 7
Values of A_i in Eq. (42) and the corresponding C constant in Eq. (39).

Material	C	A_0	A_1	A_2	A_3	A_4	A_5	θ unit	Ref.
Inconel 718	2.17E-07	0	5.4	−10.11	10.93	−6.33	1.42	Rad	[85]
SS 316	1.42E-07	−0.05065	0.04065	5.39E-04	−3.97E-05	5.14E-07	−2.07E-09	Degree	[86]

$$\lambda_L = \left(\frac{V_{SL}}{V_{SL} + V_{SG}}\right)^{0.11} \quad (48)$$

$$n = 1 - \exp\left(-0.25\frac{V_{SG}}{V_{SL}}\right) \quad (49)$$

In all the alternative models presented to this point, including the Tulsa model, the quantification of erosion for multiphase flow is performed using the mixture fluid properties. These models do not consider the multiphase-flow regimes in the erosion prediction calculations. Experiments showed that for an identical average fluid velocity in multiphase flow, different flow regimes can lead to different erosion rates up to an order of magnitude. The main flow regimes in horizontal multiphase lines are dispersed bubble, stratified, slug and annular-mist and in vertical multiphase lines are bubble, annular-mist, slug and churn flow [82,98]. McLaury et al. [99] reported that the vertical orientation is 1.6–5 times more erosive than the horizontal orientation. Among the vertical flow regimes, the severity of erosion is highest in the annular-mist flow [100]. Thus, the effect of flow regimes should be incorporated in modeling erosion for multiphase flow.

In multiphase flow, the interfacial forces between the phases, the properties of the phases, the superficial velocities, flow orientation and pipe inclination angle are parameters that influence the flow regime. For various multiphase-flow regimes, the erosion models should differ in the way they account for the characteristic particle impact velocity (V_L). In erosion models that include the effect of flow regimes, the characteristic particle impact velocity is estimated based on the physics involved in the given flow regime [82]. For example, in annular-mist flow the sand particles travelling in the gas core must pass through the thin liquid film at the pipe wall before impacting the wall and causing erosion. In slug flow, it is assumed that erosion is mainly caused by sand particles uniformly distributed in the slug body [100]. For details on how to calculate the characteristic particle impact velocity in different multiphase-flow regimes, the reader is referred to Refs. [101,102] for bubbly, Refs. [26,101–104] for annular, Refs. [26,101,105] for slug, and Refs. [100,101] for churn flow. For multiphase flow with a homogeneous flow regime such as dispersed bubble, the mixture fluid properties approach (Eqs. (44)–(46)) can be used for the erosion prediction calculations [106].

The Tulsa model can be used to estimate the erosional velocity if an allowable erosion rate (for example 5 or 10 mpy) is specified. The procedure to determine the erosional velocity is outlined as follows:

(1) Establish an allowable erosion rate (*e.g.* 5 mpy).
(2) Calculate V_L from Eq. (28) or Eq. (39) or any other erosion equation from the Tulsa model.
(3) Calculate L from Eq. (31) or Eq. (32).
(4) Make an initial guess for V_o and plug it into Eq. (34) for V_f.
(5) Plug V_f equation into Eq. (33) (or any other particle tracking equation) and solve the final equation for V_P with an initial boundary condition of $V_P = V_o$ at x = 0. If V_P at the pipe wall ($x = L - \frac{d_P}{2}$) equals to V_L found in Step 2, then the initial guess of V_o is considered as the erosional velocity. Otherwise, change the initial guess and repeat the procedure until the condition in step 5 is satisfied.

The Tulsa model has advantages over other sand erosion models explained in this paper when it comes to how it describes the erosion process. For example, it considers the reduction in the particle velocity as the particle moves through the fluid stagnation zone before impinging the pipe wall [59]; it accounts for many key factors in sand erosion including flow geometry type, size, and material; flow regime and velocity; and sand shape, size and density [82].

However, the original Tulsa model has limitations as well. The calculation of the particle impact velocity is based on a 1D particle tracking equation. In other words, only the particle velocity component along the stagnation length is considered for the calculations and the other two components that might be essential in erosion prediction are not considered. In 2010, Zhang el at. [107] used a 2D particle tracking method for the Tulsa model. They reported that the 2D model agreed very well with the experimental data from other researchers, while the 1D model over predicted for most cases. In similar research, Zhang et al. [105] showed that in single-phase flow, the 1D model underpredicted erosion caused by small particles (~20 μm), while predicted successfully for relatively large particles (> 50 μm). In slug flow, they reported that the 1D model overpredicted erosion for the large particles; however, it performed very well for the small particles. CFD simulations can be used for a more accurate estimation of the particle impact velocity by including all three flow velocity components (3D particle tracking equation) [107].

The effect of turbulent dispersion of sand particles is not considered in the original Tulsa model. This limits the model's application to relatively large sand particles (> 50–100 μm) and single-phase gas flow because large particles possess more momentum and are not affected by the turbulence as much as small particles. Also, turbulent fluctuations affect particle motion less in gas flow comparing to liquid flow [107]. Shirazi et al. [95] included the effect of turbulent flow in the Tulsa

Table 8
Parameters used in Eqs. (39) and (43).

n_1	n_2	n_3	H_v(GPa)	f	C(metric units)	Target material	conditions	Ref. (year)
1.40	1.64	2.60	1.50	1.72	1.42E-07	SS 316	Air/sand (150 μm)	[89] (2010)
0.59	3.60	2.50	1.20	5.27	1.50E-07	Al 6061	Air/sand (150 μm)	
0.50	2.50	0.50	1.20	2.19	3.28E-07	Al 6061	Air/sand (300 μm)	
1.90	0.96	35	1.10	3.25	2.55E-07	Al 6061	Air/glass beads (50 μm)	[90] (2011)
0.85	0.60	44	1.09	3.67	4.65E-07	Al 6061	Air/glass beads (150 μm)	
1.38	0.68	44	1.09	3.64	2.80E-07	Al 6061	Air/glass beads (350 μm)	
0.40	0.80	3.00	1.52	1.71	2.20E-07	SS 316	Air/sand (300 μm)	[81] (2014)
0.60	0.50	2.80	2.27	1.64	3.41E-07	Inconel 625	Air/sand (300 μm)	
0.65	1.40	1.50	2.74	3.46	(2.72 ± 0.44)E-07	22Cr	Air/sand (300 μm)	
0.50	1.40	1.20	1.92	2.05	(1.88 ± 0.79)E-07	13Cr Duplex	Air/sand (300 μm)	
0.98	1.70	2.91	1.72	4.13	(2.36 ± 0.44)E-07	1018 CS	Air/sand (300 μm)	
0.40	1.50	2.50	1.44	2.81	(2.25 ± 0.14)E-07	4130 CS	Air/sand (300 μm)	
0.60	2.20	13	1.09	5.94	(1.36 ± 1.44)E-07	Al 6061	Air/sand (300 μm)	
0.40	0.80	3.00	1.52	1.71	(3.08 ± 0.39)E-07	SS 316	Air/sand (300 μm)	[91] (2014)
0.20	0.85	0.65	1.83	1.71	4.49E-07	SS 316	Water/sand (300 μm)	[92] (2015)
0.20	0.85	0.65	1.83	1.43	4.92E-07	SS 316	Air/sand (300 μm)	[93] (2016)
1.52	8.90	0.01	1.83	18.74	2.04E-07	SS 316	Water/sand (300 μm)	
0.15	0.85	0.65	1.83	1.54	4.62E-07	SS 316	Air/sand (300 μm)	[87] (2016)
0.40	0.80	2.08	1.83	1.72	1.14E-08	SS 316	Air/sand (150 and 300 μm)	[94] (2016)

model (Eq. (28)) by introducing another velocity component that characterizes motion of eddies in the flow stream or in the turbulent boundary layer close to the wall. They claimed that this new model showed a relatively good agreement between the experimental and calculated results for single and multiphase flow, except for few cases in annular flow, which was probably because the effect of liquid film was not considered in the model [95].

The Tulsa model relies on empirical equations to account for the particle size and shape, and material target in erosion prediction calculations. However, these equations are not always accurate [69]. As shown in Table 8, for similar erodent particle and target material different C constants have been incorporated into the final erosion equation (Eq. (39)). Even with the same parameters for the impact angle function, different C constants have been considered for Eq. (39) (compare rows 7 and 14 of Table 8).

Finally, the original Tulsa model is mainly limited to simple geometries such as elbows and tees and single-phase carrier fluid such as gas or liquid [95]. For complex geometries and multiphase flow, CFD codes have been employed in the Tulsa model, primarily for calculating the particle impact velocity (V_L). The CFD-based models — CFD codes linked with empirical erosion equations — can be used for developing simplified models for erosion prediction in complex geometries and multiphase flow. Zhang et al. [107] in 2010 claimed that while CFD-based models are powerful tools, they require too much computational effort, and therefore, are not practical for engineering applications. However, with the constant advancement of CFD software packages and faster computers, CFD techniques are rapidly becoming a mainstream tool fully available to practicing engineers. Therefore, this argument may not carry as much weight today as it did 10 years ago.

7.6. Shell model

The Shell model also called the Reduced Order model was developed around 1997 based on the Tulsa model for estimating the erosion rate and the erosional velocity in multiphase flow. In the Shell model, Eq. (28) was used for the sand erosion rate calculations with two main simplifications. First, instead of Eq. (33) for calculating the impact particle velocity which requires significant numerical computation to solve, a simpler particle tracking equation was offered [59]:

$$\frac{V_P}{V_f} = \left(1 - 10.147\left(\frac{\Phi}{Re}\right) + 23.62\left(\frac{\Phi}{Re}\right)^2\right)\left(\frac{1}{1+\frac{\Phi}{6}}\right) \tag{50}$$

The two dimensionless numbers: Φ (mass ratio) and Re (particle Reynolds number) in Eq. (50) are as below [59]:

$$Re = \frac{\rho_f V_f d_P}{\mu_f} \tag{51}$$

$$\Phi = \frac{L\rho_f}{d_P \rho_P} \tag{52}$$

The second simplification was setting the total erosion rate equal to the summation of the erosion rate caused by each phase. An effective pipe diameter (D_{eff}) was defined for each phase in order to calculate the erosion rate for that phase. The following equation is the effective pipe diameter for the liquid phase:

$$D_{eff,L} = ID\left(\frac{Q_L}{Q_L + Q_G}\right)^{\frac{1}{2}} \tag{53}$$

A similar equation can be used for the gas phase [59].

The phase separation assumption was not entirely correct because for low liquid flow rates (small Q_L) like annular-mist flow, $D_{eff,L}$ will be small, which literally means there is no stagnation zone (it is a function of the diameter), while for high liquid flow rates the effect of stagnation zone will be considerable [59].

8. Comparison of erosion models

Fig. 2 uses the box-and-whisker plot format to present the ratio of calculated to experimentally measured erosion in the presence of solids. A value of 1 for the ratio (indicated on the y-axis) represents perfect agreement. Above 1 indicates that the erosion model overpredicts the

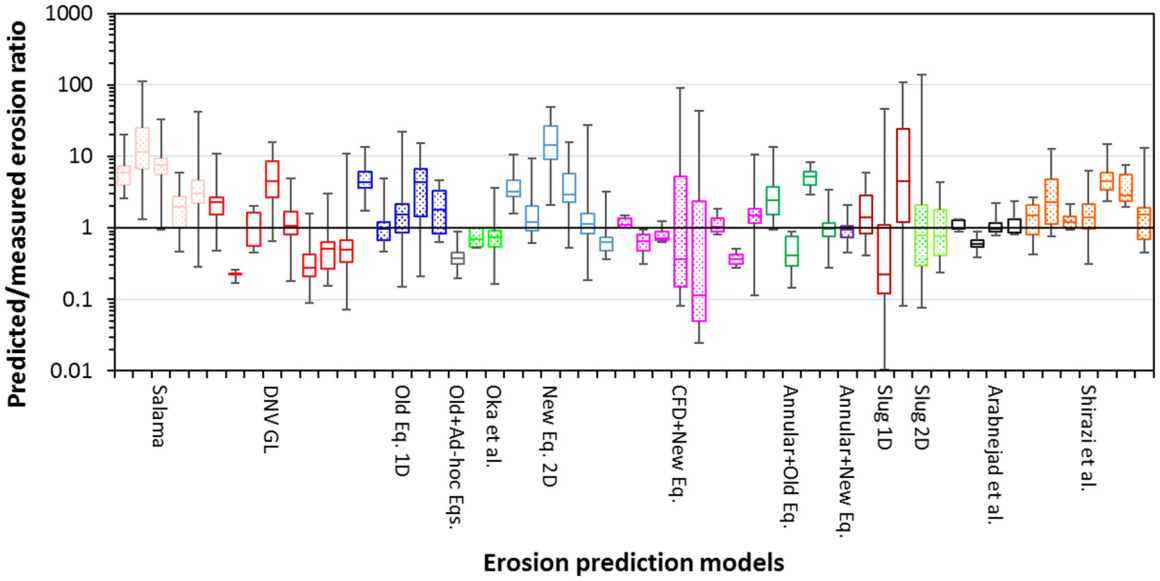

Fig. 2. The ratio of calculated to measured erosion in the presence of solids shown by box-and-whisker plots (min, quartile 1, median, quartile 3 and max). Each box represents a separate set of experimental data compared with an erosion model. 1D and 2D indicate one and two-dimensional equations of motion used in the Tulsa model, respectively. The description of each model and the Refs. data taken from: Salama: Eq. (14) [76,95,97]; DNV GL: Eqs. (18)–(27) [44,76,87,97]; Old Eq. 1D: Eq. (28), flow-regime independent [76,97]; Old + Ad-hoc Eqs.: Eq. (28) and Eqs. (47)–(49) [97]; Oka et al.: Eqs. (35)–(38) [87,97]; New Eq. 2D: Eq. (39), based on Zhang et al. [107] [76,87,97]; CFD + New Eq.: CFD codes + Eq. (39), based on Zhang et al. [85] [3,86,87,89,92,94,97]; Annular + Old Eq.: Eq. (28), based on Mazumder et al. [100,101] [26,97,103,108]; Annular + New Eq.: Eq. (39), based on Zahedi et al. [103]; Slug 1D: Eq. (28), based on Mazumder et al. [100,101] [26,105]; Slug 2D: Eq. (39), based on Zhang et al. [105]; Arabnejad et al.: based on Arabnejad et al. [69] [3,97]; Shirazi et al.: turbulent model, based on Shirazi et al. [95].

corresponding experimental data and *vice versa*. Overprediction of erosion corresponds to a lower erosional velocity limit, implying that the model is conservative. Conversely, underprediction of erosion translates to a higher erosional velocity limit, which may lead to risky decisions. The experimental values presented in Fig. 2 are generated by a statistical analysis of data gathered from various publications in the open literature. Each box corresponds to a separate set of erosion experimental data that is compared with the corresponding erosion values calculated by a given model.

Three groups of erosion calculations are shown in Fig. 2: the Salama model, the DNV GL model, and different versions of the Tulsa model. The Salama model overpredicted the experimental data in almost all cases (often by one order of magnitude or more), and hence can be considered quite conservative. The DNV GL model showed similar accuracy (within an order of magnitude); however, the underprediction was frequent and presents a potential risk as it can lead to an overestimation of the erosional velocity.

When it comes to different versions of the Tulsa model, Fig. 2 shows that both "Old Eq. 1D" and "New Eq. 2D" models tended to overpredict erosion, performing in general similarly to Salama model. However, the dispersion of the "Old Eq. 1D" predictions was less than that for the "New Eq. 2D" model, suggesting that it is somewhat more accurate. This conclusion is at odds with Zhang et al. [107]'s claim that the "New Eq. 2D" model predicts erosion behavior much better than the "Old Eq. 1D" model. Recall that the "Old + Ad-hoc Eqs." model is the same as the "Old Eq. 1D" model except that Eqs. (47)–(49) are used instead of Eq. (46) for calculating the fluid bulk velocity. The single data set used for the evaluation of the "Old + Ad-hoc Eqs." model shows that it underpredicted the experimental results. However, more data are required to make a more accurate conclusion about the accuracy of this model. Even though the Oka et al. model appears to be relatively accurate, it underpredicted most of the erosion data, which makes the model less safe for practical purposes.

The "CFD + New Eq." model refers to the Tulsa model in which CFD codes were used for flow modeling and particle tracking, and Eq. (39) was used for erosion prediction. As mentioned above, this type of model is the most commonly used version of the Tulsa model as is indicated in the open literature. The Zhang et al. [85] model is the basis of the "CFD + new Eq." model. The exact CFD packages used in the "CFD + New Eq." models are not explicitly referenced in the original publications. It is possible that the boxes in Fig. 2 for the "CFD + New Eq." models are based on different CFD packages, such as FLUENT, CFX or STAR-CCM+, which may be the source of difference in the results. Fig. 2 shows that the "CFD + New Eq." models underpredicted the experimental data for the majority of cases (considering the median) and in some cases the spread was unacceptably large. Several researchers reported that the CFD-based Tulsa models underpredicted the experimental erosion data [85,86,89,92], *e.g.* Zhang et al. [85] and Okita [89] mentioned that the CFD-based Tulsa model underpredicted the experimental data as the viscosity of the carrier fluid increases.

When it comes to different multiphase flow regimes, both Annular models predicted the experimental data relatively well with an order of magnitude accuracy. For both Slug models, the ratio of calculated to measured erosion scattered significantly, with the Slug 2D model being more accurate than the Slug 1D model.

In summary, among all the models presented in Fig. 2, it appears that the Arabnejad et al. [69] and Shirazi et al. [95] models were the most accurate and suitable models for estimating the erosional velocity, which is not a surprise as they are the most recent models presented by this group.

Some of the erosion models discussed above were used for a hypothetical case (with conditions listed in Table 9) to compare the erosional velocity calculated by them with that estimated by the API RP 14E equation.

Fig. 3 shows the results of such a comparison for a given allowable erosion rate of 5 mpy. Above and to the right of each curve indicates velocities resulting in the erosion rate being greater than 5 mpy, and *vice versa*. Where the complete descriptions of the erosion models were given in the open literature, *i.e.* for the API RP 14E, Salama, and DNV GL models, the models were recreated and used for the erosional velocity calculations. For the Tulsa model, the SPPS 1D software version 5.3. was used. For the Shirazi et al. (turbulent) model, because of the incomplete information available in the public domain, data were taken directly from the source publication [95]. The comparison for the Shirazi et al. model might not be completely correct because not all the input conditions listed in Table 9 were mentioned in the source publication.

The comparison shows that the API RP 14E equation is the most conservative model for high liquid superficial velocities (flow lines with a considerable amount of liquid). At these conditions, the API RP 14E erosional velocity amounting to a total velocity of approximately 10–20 ft/s corresponds roughly to the transition from slug to dispersed bubble flow, as shown in the flow regime map in Fig. 4 (and as gray dotted lines in Fig. 3), generated for the same conditions. While this might be a coincidence, it makes little sense to limit the velocity so that the flow regime does not transit from slug (which is generally considered to be the most violent) to dispersed bubble (which is thought as one of the most benign). At high liquid superficial velocities, the Salama model allows the highest operating velocities, yet at unrealistic levels, where other operational restrictions must apply. The DNV GL, Tulsa and Shirazi et al. models predict the erosional velocity somewhere in between the API RP 14E equation and the Salama model.

Conversely, at high superficial gas velocities and low superficial liquid velocities (flow lines with a considerable amount of gas and a small amounts of liquid), the API RP 14E equation allows the highest velocity and is actually the least conservative model, while the Salama and Shirazi et al. models are the most conservative models, with the others being in between. This is probably the reason for recommending 50% of the API RP 14E erosional velocity as the safe operating velocity for gas pipelines [109]. From comparisons with the flow regime map (Fig. 4) it appears that most of the models restrict the transition to the annular-mist flow regime, which is logical as the high gas velocities may lead to significant levels of droplet and sand impingement. However, this could be just a coincidence, as most of the models do not explicitly account for the effect of various two-phase flow regimes.

Table 9
Parameters for calculation of the erosional velocity.

Parameter	Value	Unit	Description
Operating pressure	514.7	psia	–
Operating temperature	100	°F	–
Carrier fluids	–	–	Water and methane
Water cut	1	–	Ratio of water to total liquid
Gas specific gravity	0.55	–	S_g
Gas density	1.445	lb/ft^3	–
Gas viscosity	0.033	cp	–
Liquid specific gravity	1	–	S_l
Liquid density	62.01	lb/ft^3	–
Liquid viscosity	0.682	cp	–
Gas compressibility	0.998	–	Z
Gas-liquid surface tension	7.21	dyne/cm	–
Pipe geometry	–	–	Seamless long radius elbow
Material	–	–	Carbon steel
Material density	486.94	lb/ft^3	–
Pipe diameter	4	in	–
Radius of curvature	5	–	–
Material hardness	140	B	Brinell
Pipe roughness	20	μm	–
Sand feed rate	10	lb/day	–
Sand size	150	μm	–
Sand shape	–	–	Semi-rounded
Sand density	162.31	lb/ft^3	–

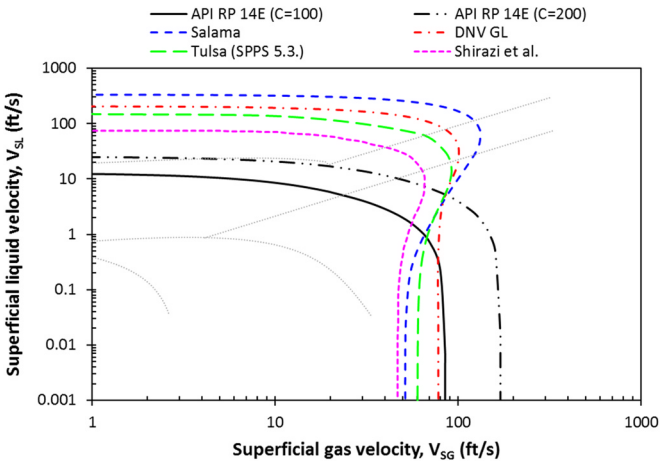

Fig. 3. Comparison of erosional velocity curves calculated by the API RP 14 equation and other models based on conditions listed in Table 9. Data for the Shirazi et al. model are taken from Ref. [95]. The gray dotted lines present the flow regime map shown in Fig. 4. For the API RP 14E equation, the ideal gas law was used to convert the gas velocity at operating conditions to that at standard conditions and the gas/liquid ratio at standard conditions (R) was assumed to be equal to $5.61(V_{sg}/V_{sl})$ (see the Supplementary Materials for details on calculations).

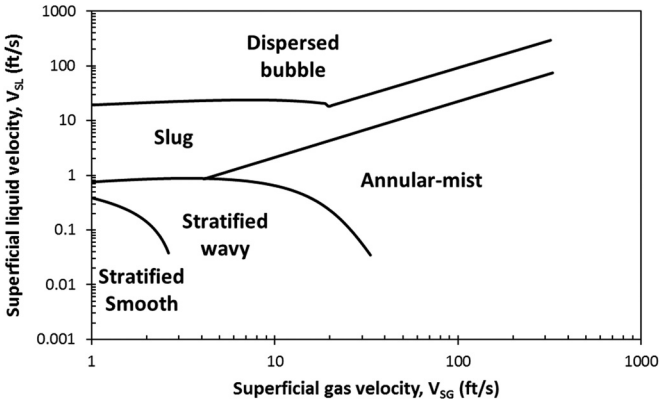

Fig. 4. The flow regime map for a 4-in vertical pipe operating at conditions listed in Table 9. Calculated with MULTICORP™ 5.5.0.

9. Current oilfield approaches

Current oilfield practices generally combine several of the approaches discussed previously:

- For non-corrosive fluids without solids, any restrictions due to possible erosion are not a limiting factor, *i.e.* the API RP 14E equation that is actually defined for this type of service, is not used.
- The effect of flow for the case of transportation of corrosive fluids without solids (FIC/FAC scenario) are covered by existing corrosion models (such as MULTICORP™, OLI Systems, ECE®, Thermo-Calc, *etc.)*.
- For non-corrosive fluids with solids (erosion scenario), instead of using the API RP 14E equation with a reduced c-factor, the alternatives, such as the DNV GL or the Tulsa erosion models are sometimes used. In special cases with more complicated geometries, more advanced CFD models are used.
- For corrosive fluids with solids (case of erosion-corrosion), specific studies are often performed or field experience may be applied when available. Although researchers have been trying to model the combined process of erosion and corrosion [11,67,110–115], since the mechanism for erosion-corrosion is still not fully understood this area needs further improvement. Rules of thumb and simple empirical guidelines are used in most applications. These often amount to specifying the erosional velocity directly or using simple criteria in the forms of decision tables or flowcharts on how to determine the limiting velocity. The rules and guidelines differ from company to company. They are based on operational conditions such as concentration of solids, type of service, corrosiveness of the fluid, and presence of corrosion inhibitors.

10. Conclusions

- The widespread use of the API RP 14E erosional velocity equation is a result of its simplicity and requiring little in the way of inputs. However, the API RP 14E equation does not account for most of the factors important in erosion, FIC/FAC and erosion-corrosion.
- The origin of the API RP 14E erosional velocity equation remains unclear. The theoretical explanations (*e.g.* energy balance, Bernoulli equation, liquid droplet impingement, and corrosion inhibitor/product removal) that supposedly underpin the derivation of the API RP 14E equation do not seem to properly justify its form. The alternative explanations involving anecdotal evidence on empirical origin of the API RP 14E equation are even less convincing.
- There is a problematic assumption (often implicit) that the API RP 14E equation can be used as a means of generalizing observed empirical erosion, FIC/FAC or erosion-corrosion data to derive safe operational velocities for a broad variety of conditions, usually outside operational or experimental ranges. This assumption ignores the fact that the mechanism and the rate of degradation can be very different (by orders of magnitude) depending on type of service or even within the same type of service.
- The API RP 14E equation cannot be simply applied to all kinds of conditions by just modifying the c-factor, assuming that it is universally valid and it will give reasonable values.
- Despite its widespread use, the API RP 14E equation has many limitations. Probably the most significant is that it does not provide any quantitative guidelines for limiting the velocity in the two most critical scenarios: when solid particles are present in the production fluids (erosion) and when erosion and corrosion are both an issue (erosion-corrosion). A reduction in the c-factor is recommended by API RP 14E, although it is unclear how to obtain the exact value.
- Some of the alternative approaches overlap with and in some aspects go beyond the narrow application range of the API RP 14E erosional velocity equation. Examples are the NORSOK P-002 standard [68] and to some extent the recommendations of Svedeman and Arnold [63]. In other cases, the alternatives focus on how to derive velocity limits in the presence of solid particles, beyond just arbitrarily using the API RP 14E erosional velocity equation with a smaller c-factor. The best-known examples are the Salama model, the DNV GL model, and various versions of the Tulsa model.
- When it comes to the complicating effect of combined erosion-corrosion attack, researchers have been pursuing the so called erosion-corrosion mapping approach [66,110,112]. However, in the applications, rules-of-thumb and simple empirical guidelines are used in most cases.

Acknowledgments

The authors would like to gratefully acknowledge the constructive help of Dr. Michel Bonis (TOTAL); Dr. Bruce Brown, Dr. David Young, and Dr. Luciano Paolinelli (Institute for Corrosion and Multiphase Technology); Mr. Kamal Pakdaman (BACO for Oil Industry Construction, Basra), and Mr. Hossein Jafari (Iranian Offshore Engineering and Construction Company) during the writing of this review paper.

Appendix A. Supporting information

Supplementary data associated with this article can be found in the online version at https://doi.org/10.1016/j.wear.2019.01.119.

References

[1] B.S. McLaury, J. Wang, S.A. Shirazi, J.R. Shadley, E.F. Rybicki, Solid particle erosion in long radius elbows and straight pipes, in: Soc. Pet. Eng., 1997. https://doi.org/10.2118/38842-MS.

[2] M.M., Salama, E.S., Venkatesh, Evaluation of API RP 14E erosional velocity limitations for offshore gas wells, in: Proceedings of the Offshore Technology Conference, Houston, TX, 1983: Paper No. OTC-4485-MS. 〈https://doi.org/10.4043/4485-MS〉.

[3] H. Arabnejad, A. Mansouri, S.A. Shirazi, B.S. McLaury, Abrasion erosion modeling in particulate flow, Wear 376–377 (Part B) (2017) 1194–1199, https://doi.org/10.1016/j.wear.2017.01.042.

[4] D. Lusk, M. Gupta, K. Boinapally, Armoured against corrosion, Hydrocarb. Eng. (2008).

[5] A. Thiruvengadam, Erosion, Wear, and Interfaces with Corrosion, ASTM International, Philadelphia, PA, 1982.

[6] F.J. Heymann, Liquid impingement erosion, in: Frict. Lubr. Wear Technol. American Society for Metals International, 1992, pp. 221–232.

[7] R.J.K. Wood, Erosion–corrosion interactions and their effect on marine and offshore materials, Wear 261 (2006) 1012–1023, https://doi.org/10.1016/j.wear.2006.03.033.

[8] D.C. Silverman, Rotating cylinder electrode — geometry relationships for prediction of velocity-sensitive corrosion, Corrosion 44 (1988) 42–49, https://doi.org/10.5006/1.3582024.

[9] E. Heitz, Chemo-mechanical effects of flow on corrosion, Corrosion 47 (1991) 135–145, https://doi.org/10.5006/1.3585229.

[10] K.J. Kennelley, R.H. Hausler, D.C. Silverman, Flow-Induced Corrosion: Fundamental Studies and Industry Experience, NACE, Houston, TX, 1992.

[11] J.R. Shadley, S.A. Shirazi, E. Dayalan, E.F. Rybicki, Prediction of erosion-corrosion penetration rate in a carbon dioxide environment with sand, Corrosion 54 (1998) 972–978, https://doi.org/10.5006/1.3284819.

[12] R. Barker, X. Hu, A. Neville, S. Cushnaghan, Flow-induced corrosion and erosion-corrosion assessment of carbon steel pipework in oil and gas production, in: Corrosion, NACE International, Houston, TX, 2011, p. 11245.

[13] M.M. Stack, B.D. Jana, S.M. Abdelrahman, 6- Models and mechanisms of erosion–corrosion in metals, in: Proceedings of the Tribocorrosion Passive Met. Coat., 1st ed., Woodhead Publishing, 2011, pp. 153–187. 〈https://doi.org/10.1533/9780857093738.1.153〉.

[14] R.J.K. Wood, S.P. Hutton, The synergistic effect of erosion and corrosion: trends in published results, Wear 140 (1990) 387–394, https://doi.org/10.1016/0043-1648(90)90098-U.

[15] R. Malka, S. Nesic, D.A. Gulino, Erosion–corrosion and synergistic effects in disturbed liquid-particle flow, Wear 262 (2007) 791–799, https://doi.org/10.1016/j.wear.2006.08.029.

[16] M.M. Stack, S. Zhou, R.C. Newman, Identification of transitions in erosion-corrosion regimes in aqueous environments, Wear 186–187 (1995) 523–532, https://doi.org/10.1016/0043-1648(95)07175-X.

[17] S. Hassani, K.P. Roberts, S.A. Shirazi, J.R. Shadley, E.F. Rybicki, C. Joia, Flow loop study of NaCl concentration effect on erosion, corrosion, and erosion-corrosion of carbon steel in CO_2-saturated systems (026001.1-026001.9), Corrosion 68 (2012), https://doi.org/10.5006/1.3683229.

[18] Y. Zheng, Z. Yao, X. Wei, W. Ke, The synergistic effect between erosion and corrosion in acidic slurry medium, Wear 186–187 (1995) 555–561, https://doi.org/10.1016/0043-1648(95)07132-6.

[19] S. Hassani, K.P. Roberts, S.A. Shirazi, J.R. Shadley, E.F. Rybicki, C. Joia, A new approach for predicting inhibited erosion-corrosion in CO_2-saturated oil/brine flow condition, SPE Prod. Oper. 28 (2013) 135–144, https://doi.org/10.2118/155136-PA.

[20] S. Hassani, K.P. Roberts, S.A. Shirazi, J.R. Shadley, E.F. Rybicki, C. Joia, Characterization and prediction of chemical inhibition performance for erosion-corrosion conditions in sweet oil and gas production, Corrosion 68 (2012) 885–896, https://doi.org/10.5006/0546.

[21] H. Arabnejad, S.A. Shirazi, B.S. McLaury, J.R. Shadley, Calculation of Erosional Velocity Due to Liquid Droplets with Application to Oil and Gas Industry Production, in: Society of Petroleum Engineers, New Orleans, LA, 2013, , https://doi.org/10.2118/166423-MS.

[22] J.R. Shadley, E.F. Rybicki, S.A. Shirazi, E. Dayalan, Velocity guidelines for avoiding erosion-corrosion damage in sweet production with sand, J. Energy Resour. Technol. 120 (1998) 78–83, https://doi.org/10.1115/1.2795014.

[23] S.A. Shirazi, B.S. McLaury, J.R. Shadley, E.F. Rybicki, Generalization of the API RP 14E guideline for erosive services, J. Pet. Technol. 47 (1995) 693–698, https://doi.org/10.2118/28518-PA.

[24] M.M. Salama, An alternative to API 14E erosional velocity limits for sand laden fluids, J. Energy Resour. Technol. 122 (2000) 71–77, https://doi.org/10.4043/8898-MS.

[25] API RP 14E, recommended practice for design and installation of offshore production platform piping systems, American Petroleum Institute, 5th ed., 1991.

[26] B.S. McLaury, S.A. Shirazi, E.F. Rybicki, Sand erosion in multiphase flow for slug and annular flow regimes, in: Corrosion, NACE International, San Antonio, TX, 2010, p. 10377.

[27] H. Mansoori, F. Esmaeilzadeh, D. Mowla, A.H. Mohammadi, Case study: production benefits from increasing C-values, Oil Gas J. (2013).

[28] S.R. Mofrad, Erosional velocity limit, 2014.

[29] R. Russell, S. Shirazi, J. Macrae, A New Computational Fluid Dynamics Model to Predict Flow Profiles and Erosion Rates in Downhole Completion Equipment, in: Society of Petroleum Engineers, Houston, TX, 2004, , https://doi.org/10.2118/90734-MS.

[30] H. Arabnejad, S.A. Shirazi, B.S. McLaury, J.R. Shadley, A Guideline to Calculate Erosional Velocity Due to Liquid Droplets for Oil and Gas Industry, in: Society of Petroleum Engineers, Amsterdam, Netherlands, 2014.

[31] M.M. Salama, Erosion velocity limits for water injection systems, Mater. Perform. 32 (1993) 44–49.

[32] J.M. Coulson, J.F. Richardson, Chemical Engineering, Vol. 1: SI Units, 3rd ed., Pergamon Press, 1977.

[33] U. Lotz, Velocity effects in flow induced corrosion, in: Corrosion, NACE International, Las Vegas, NV, 1990, p. 27.

[34] C.E. Brennen, Chapter 5- Cavitation parameters and inception, in: Hydrodynamics of Pumps, Cambridge University Press, 2011, pp. 55–77, , https://doi.org/10.1017/CBO9780511976728.007.

[35] M. Dular, B. Stoffel, B. Sirok, Development of a cavitation erosion model, Wear 261 (2006) 642–655, https://doi.org/10.1016/j.wear.2006.01.020.

[36] W. Li, B.F.M. Pots, X. Zhong, S. Nesic, Inhibition of CO_2 corrosion of mild steel – Study of mechanical effects of highly turbulent disturbed flow, Corros. Sci. 126 (2017) 208–226, https://doi.org/10.1016/j.corsci.2017.07.003.

[37] S. Hattori, M. Takinami, Comparison of cavitation erosion rate with liquid impingement erosion rate, Wear 269 (2010) 310–316, https://doi.org/10.1016/j.wear.2010.04.020.

[38] F. Cheng, W. Ji, C. Qian, J. Xu, Cavitation bubbles dynamics and cavitation erosion in water jet, Results Phys. 9 (2018) 1585–1593, https://doi.org/10.1016/j.rinp.2018.05.002.

[39] T. Shakouchi, K. Kinoshita, K. Tsujimoto, T. Ando, Flow-accelerated corrosion in pipe wall downstream of orifice for water and air-water bubble flows, J. Flow. Control Meas. Vis. 04 (2016) 93, https://doi.org/10.4236/jfcmv.2016.43009.

[40] B. Craig, Critical velocity examined for effects of erosion-corrosion, Oil Gas J. 83 (1985) 99–100.

[41] J.S. Smart, The meaning of the API RP 14E formula for erosion corrosion in oil and gas production, in: Corrosion, NACE International, Cincinnati, OH, 1991, p. 468.

[42] H. Arabnejad, A. Mansouri, S.A. Shirazi, B.S. McLaury, J.R. Shadley, Erosion-corrosion study of oil-field materials due to liquid impact, in: Corrosion, NACE International, Dallas, TX, 2015, p. 6136.

[43] D.M. Deffenbaugh, J.C. Buckingham, A Study of the Erosional Corrosional Velocity Criterion for Sizing Multi-phase Flow Lines, Phase I, Southwest Research Institute, Reston, VA, 1989.

[44] DNVGL-RP-O501, recommended practice: managing sand production and erosion, Det Norske Veritas, 2015.

[45] M.H. Chaudhry, Applied Hydraulic Transients, 3rd ed., Springer Science & Business Media, 2013.

[46] R.H. Hausler, C. Consulta, G. Schmitt, Hydrodynamic and flow effects on corrosion inhibition, in: Corrosion, NACE International, New Orleans, LA, 2004, p. 04402.

[47] Y. Xiong, B. Brown, B. Kinsella, S. Nesic, A. Pailleret, Atomic force microscopy study of the adsorption of surfactant corrosion inhibitor films, Corrosion 70 (2013) 247–260, https://doi.org/10.5006/0915.

[48] W. Li, B.F.M. Pots, B. Brown, K.E. Kee, S. Nesic, A direct measurement of wall shear stress in multiphase flow—Is it an important parameter in CO_2 corrosion of carbon steel pipelines? Corros. Sci. 110 (2016) 35–45, https://doi.org/10.1016/j.corsci.2016.04.008.

[49] S. Nesic, Effects of multiphase flow on internal CO_2 corrosion of mild steel pipelines, Energy Fuels 26 (2012) 4098–4111, https://doi.org/10.1021/ef3002795.

[50] J.S. Smart, A review of erosion corrosion in oil and gas production, in: Corrosion, NACE International, Las Vegas, NV, 1990, p. 10.

[51] J.A. Keeth, Some corrosion problems encountered in steam plant operations, Corrosion 11 (1946) 101–124.

[52] P. Andrews, T.F. Illson, S.J. Matthews, Erosion–corrosion studies on 13 Cr steel in gas well environments by liquid jet impingement, Wear 233–235 (1999) 568–574, https://doi.org/10.1016/S0043-1648(99)00228-8.

[53] M.J. Castle, D.T. Teng, Extending gas well velocity limits: problems and solutions, in: Proceedings of the Soc. Pet. Eng. SPE, Perth, Western Australia: 1991, pp. 135–144.

[54] R. Heidersbach, Velocity Limits for Erosion-Corrosion, in: Dallas, TX, 1985.

[55] C.C. Patton, Are we out of the iron age yet? in: Corrosion, NACE International, Houston, TX, 1993, p. 93056.

[56] D. Panic, J. House, Challenging conventional erosional velocity limitations for high rate gas wells, in: 2009, p. 6.

[57] M.A. Ariana, F. Esmaeilzadeh, D. Mowla, Beyond the limitations of API RP-14E erosional velocity - a field study for gas condensate wells, Phys. Chem. Res. 6 (2018) 193–207, https://doi.org/10.22036/pcr.2017.93963.1403.

[58] Annual report to Alaska department of environmental conservation: commitment to corrosion monitoring, Corrosion, Inspection and Chemicals (CIC) Group, BP Exploration (Alaska) Inc., 2002.

[59] K. Jordan, Erosion in multiphase production of oil & gas, in: Corrosion, NACE International, San Diego, California, 1998, p. 5834.

[60] M. Bonis, Private technical communication, TOTAL, 2018.

[61] J.H. Gerretsen, A. Visser, Inhibitor performance under liquid droplet impingement conditions in CO_2-containing environment, Corros. Sci. 34 (1993) 1299–1310, https://doi.org/10.1016/0010-938X(93)90089-Y.

[62] API Specification 5CT, Specification for Casing and Tubing, 10th ed., American Petroleum Institute, 2018.
[63] S.J. Svedeman, K.E. Arnold, Criteria for sizing multiphase flowlines for erosive/corrosive service, SPE Prod. Facil 9 (1994) 74–80, https://doi.org/10.2118/26569-PA.
[64] U.R. Richard, Sand and Fines in Multiphase Oil and Gas Production (Master's thesis), Norwegian University of Science and Technology, Trondheim, Norway, 2013.
[65] A.T. Salazar, Erosional velocity limitations for oil and gas wells - extracted from Neotec Wellflow Manual, 2012.
[66] C.B. Burson-Thomas, R.J.K. Wood, Developments in erosion–corrosion over the past 10 Years, J. Bio- Tribo Corros. 3 (2017) 14, https://doi.org/10.1007/s40735-017-0073-4.
[67] M.M. Stack, B.D. Jana, Modelling particulate erosion–corrosion in aqueous slurries: some views on the construction of erosion–corrosion maps for a range of pure metals, Wear 256 (2004) 986–1004, https://doi.org/10.1016/j.wear.2003.09.004.
[68] NORSOK P-002, Process system design (Revision 1), Standards Norway (SN), 2014.
[69] H. Arabnejad, A. Mansouri, S.A. Shirazi, B.S. McLaury, Development of mechanistic erosion equation for solid particles, Wear 332–333 (2015) 1044–1050, https://doi.org/10.1016/j.wear.2015.01.031.
[70] International Standard, ISO 13703: petroleum and natural gas industries—design and installation of piping systems on offshore production platforms, 2000.
[71] Specifications for salt water piping systems in ships (BS MA18: 1973), British Standards Institution.1976.
[72] A.T.J. Bourgoyne, Experimental study of erosion in diverter systems due to sand production, in: Soc. Pet. Eng., 1989, pp. 807–816. https://doi.org/10.2118/18716-MS.
[73] S.J. Svedeman, A Study of the Erosional/Corrosional Velocity Criterion for Sizing Multiphase Flow Lines, Phase II, Southwest Research Institute, Reston, VA, 1990.
[74] A. Huser, O. Kvernvold, Prediction of sand erosion in process and pipe components, in: Proceedings of the 1st North Am. Conference Multiph. Technol., Banff, Canada: 1998: pp. 217–227.
[75] I. Finnie, Erosion of surfaces by solid particles, Wear 3 (1960) 87–103, https://doi.org/10.1016/0043-1648(60)90055-7.
[76] H. Arabnejad, A. Mansouri, S.A. Shirazi, B.S. McLaury, Evaluation of solid particle erosion equations and models for oil and gas industry applications, in: Proceedings of the Soc. Pet. Eng., Society of Petroleum Engineers, Houston, TX: 2015, Paper No. SPE-174987-MS. ⟨https://doi.org/10.2118/174987-MS⟩.
[77] B.S. McLaury, S.A. Shirazi, J.R. Shadley, E.F. Rybicki, A particle tracking method to predict sand erosion threshold velocities in elbows and tees, in: Proceedings of the ASME Fluids Eng. Div., Lake Tahoe, Nevada, 1:994, pp. 145–154.
[78] S.A. Shirazi, J.R. Shadley, B.S. McLaury, E.F. Rybicki, A procedure to predict solid particle erosion in elbows and tees, J. Press. Vessel Technol. 117 (1995) 45–52, https://doi.org/10.1115/1.2842089.
[79] B.S. McLaury, A Model to Predict Solid Particle Erosion in Oilfield Geometries (Master's thesis), The University of Tulsa, Tulsa, OK, 1993.
[80] B.S. McLaury, S.A. Shirazi, An alternative method to API RP 14E for predicting solids erosion in multiphase flow, J. Energy Resour. Technol. 122 (2000) 115–122.
[81] R.E. Vieira, Sand Erosion Model Improvement for Elbows in Gas Production, Multiphase Annular and Low-liquid Flow (Ph.D. thesis), The University of Tulsa, Tulsa, OK, 2014.
[82] M. Parsi, K. Najmi, F. Najafifard, S. Hassani, B.S. McLaury, S.A. Shirazi, A comprehensive review of solid particle erosion modeling for oil and gas wells and pipelines applications, J. Nat. Gas Sci. Eng. 21 (2014) 850–873, https://doi.org/10.1016/j.jngse.2014.10.001.
[83] Y.I. Oka, K. Okamura, T. Yoshida, Practical estimation of erosion damage caused by solid particle impact, Wear 259 (2005) 95–101, https://doi.org/10.1016/j.wear.2005.01.039.
[84] Y.I. Oka, T. Yoshida, Practical estimation of erosion damage caused by solid particle impact: part 2: mechanical properties of materials directly associated with erosion damage, Wear 259 (2005) 102–109, https://doi.org/10.1016/j.wear.2005.01.040.
[85] Y. Zhang, E.P. Reuterfors, B.S. McLaury, S.A. Shirazi, E.F. Rybicki, Comparison of computed and measured particle velocities and erosion in water and air flows, Wear 263 (2007) 330–338, https://doi.org/10.1016/j.wear.2006.12.048.
[86] A. Mansouri, S.A. Shirazi, B.S. McLaury, Experimental and numerical investigation of the effect of viscosity and particle size on the erosion damage caused by solid particles, (2014) V01DT31A002. ⟨https://doi.org/10.1115/FEDSM2014-21613⟩.
[87] R.E. Vieira, A. Mansouri, B.S. McLaury, S.A. Shirazi, Experimental and computational study of erosion in elbows due to sand particles in air flow, Powder Technol. 288 (2016) 339–353, https://doi.org/10.1016/j.powtec.2015.11.028.
[88] S. TorabzadehKhorasani, Erosion Experiments and Calculations in Gas and Liquid Impacts Varying Particle Size and Viscosity (Master's thesis), The University of Tulsa, Tulsa, OK, 2009.
[89] R. Okita, Effects of Viscosity and Particle Size on Erosion Measurements and Predictions (Master's thesis), The University of Tulsa, Tulsa, OK, 2010.
[90] S.A. Nidasanametla, Effect of Viscosity, Particle Size and Shape on Erosion Measurements and Predictions (Master's thesis), The University of Tulsa, Tulsa, OK, 2011.
[91] R.E. Vieira, N.R. Kesana, S.A. Shirazi, B.S. McLaury, Experiments for sand erosion model improvement for elbows in gas production, low-liquid loading and annular flow conditions, in: Corrosion, NACE International, San Antonio, TX, 2014, p. 4325.
[92] A. Mansouri, M. Mahdavi, S.A. Shirazi, B.S. McLaury, Investigating the effect of sand concentration on erosion rate in slurry flows, in: Corrosion, NACE International, Dallas, TX, 2015, p. 6130.
[93] A. Mansouri, A Combined CFD-Experimental Method for Developing an Erosion Equation for Both Gas-sand and Liquid-sand Flows (Ph.D. thesis), The University of Tulsa, Tulsa, OK, 2016.
[94] P. Zahedi, S. Karimi, M. Mahdavi, B.S. McLaury, S.A. Shirazi, Parametric analysis of erosion in 90° and long radius bends, in: Proceedings of the Fluid Eng. Div. Summer Meet., Washington, DC, 2016, Paper No. FEDSM2016-7735. ⟨https://doi.org/10.1115/FEDSM2016-7735⟩.
[95] S.A. Shirazi, B.S. McLaury, H. Arabnejad, A semi-mechanistic model for predicting sand erosion threshold velocities in gas and multiphase flow production, in: Soc. Pet. Eng., Dubai, UAE, 2016. https://doi.org/10.2118/181487-MS.
[96] Y. Zhang, Application and Improvement of Computational Fluid Dynamics (CFD) in Solid Particle Erosion Modeling (Ph.D. thesis), The University of Tulsa, Tulsa, OK, 2006.
[97] M. Parsi, M. Kara, P. Sharma, B.S. McLaury, S.A. Shirazi, Comparative study of different erosion model predictions for single-phase and multiphase flow conditions, in: Proceedings of the Offshore Technology Conference, Houston, TX, 2016, Paper. No. OTC-27233-MS. ⟨https://doi.org/10.4043/27233-MS⟩.
[98] A.M. Ansari, N.D. Sylvester, C. Sarica, O. Shoham, J.P. Brill, A comprehensive mechanistic model for upward two-phase flow in wellbores, SPE Prod. Facil 9 (1994) 143–151, https://doi.org/10.2118/20630-PA.
[99] B.S. McLaury, V. Viswanathan, S.A. Shirazi, Q.H. Mazumder, Effect of upstream pipe orientation on erosion/corrosion in bends for annular flow, in: Corrosion, NACE International, San Diego, Ca, 2006, p. 06572.
[100] Q.H. Mazumder, S.A. Shirazi, B.S. McLaury, A mechanistic model to predict erosion in multiphase flow in elbows downstream of vertical pipes, in: Corrosion, NACE International, New Orleans, LA, 2004, p. 04662.
[101] Q.H. Mazumder, S.A. Shirazi, B.S. McLaury, J.R. Shadley, E.F. Rybicki, Development and validation of a mechanistic model to predict solid particle erosion in multiphase flow, Wear 259 (2005) 203–207, https://doi.org/10.1016/j.wear.2005.02.109.
[102] X. Chen, B.S. McLaury, S.A. Shirazi, A comprehensive procedure to estimate erosion in elbows for gas/Liquid/sand multiphase flow, J. Energy Resour. Technol. 128 (2005) 70–78, https://doi.org/10.1115/1.2131885.
[103] P. Zahedi, R.E. Vieira, S.A. Shirazi, B.S. McLaury, Liquid film thickness and erosion of elbows in gas-liquid annular flow, in: Corrosion, NACE International, Vancouver, BC, 2016, p. 7711.
[104] L.B. Fore, A.E. Dukler, The distribution of drop size and velocity in gas-liquid annular flow, Int. J. Multiph. Flow 21 (1995) 137–149, https://doi.org/10.1016/0301-9322(94)00061-N.
[105] Y. Zhang, B.S. McLaury, S.A. Shirazi, E.F. Rybicki, S. Nesic, Predicting sand erosion in slug flows using a two-dimensional mechanistic model, in: Corrosion, NACE International, Houston, TX, 2011, p. 11243.
[106] S.A. Shirazi, B.S. McLaury, J.R. Shadley, K.P. Roberts, Erosion-corrosion in oil and gas pipelines, in: Oil Gas Pipelines, Wiley-Blackwell, 2015, pp. 399–422, , https://doi.org/10.1002/9781119019213.ch28.
[107] Y. Zhang, B.S. McLaury, S.A. Shirazi, E.F. Rybicki, A two-dimensional mechanistic model for sand erosion prediction including particle impact characteristics, in: Corrosion, NACE International, San Antonio, TX, 2010, p. 10378.
[108] Q.H. Mazumder, S.A. Shirazi, B.S. McLaury, Prediction of solid particle erosive wear of elbows in multiphase annular flow-model development and experimental validations (023001.1-023001.10), J. Energy Resour. Technol. 130 (2008), https://doi.org/10.1115/1.2824284.
[109] E.S. Menon, Gas Pipeline Hydraulics, Taylor & Francis, 2005, https://doi.org/10.1201/9781420038224.
[110] F.M. Al-Mutahar, K.P. Roberts, S.A. Shirazi, E.F. Rybicki, J.R. Shadley, Modeling and experiments of $FeCO_3$ scale growth and removal for erosion-corrosion conditions, in: Corrosion, NACE International, Salt Lake City, UT, 2012, p. 1132.
[111] G.H. Al-Aithan, F.M. Al-Mutahar, J.R. Shadley, S.A. Shirazi, E.F. Rybicki, K.P. Roberts, A mechanistic erosion-corrosion model for predicting iron carbonate ($FeCO_3$) scale thickness in a CO_2 environment with sand, in: Corrosion, NACE International, San Antonio, TX, 2014, p. 3854.
[112] M.M. Stack, S.M. Abdelrahman, B.D. Jana, A new methodology for modelling erosion–corrosion regimes on real surfaces: gliding down the galvanic series for a range of metal-corrosion systems, Wear 268 (2010) 533–542, https://doi.org/10.1016/j.wear.2009.09.013.
[113] J. Postlethwaite, S. Nesic, G. Adamopoulos, D.J. Bergstrom, Predictive models for erosion-corrosion under disturbed flow conditions, Corros. Sci. 35 (1993) 627–633, https://doi.org/10.1016/0010-938X(93)90197-O.
[114] S. Nesic, J. Postlethwaite, A predictive model for localized erosion—corrosion, Corrosion 47 (1991) 582–589, https://doi.org/10.5006/1.3585295.
[115] A. Keating, S. Nesic, Numerical prediction of erosion-corrosion in bends, Corrosion 57 (2001) 621–633, https://doi.org/10.5006/1.3290389.